

A Primer on Instantons in QCD

Hilmar Forkel
Institut für Theoretische Physik, Universität Heidelberg,
Philosophenweg 19, D-69120 Heidelberg
Germany

August 2000

These are the extended notes of a set of lectures given at the “12th Workshop on Hadronic Interactions” at the IF/UERJ, Rio de Janeiro (31. 5. - 2. 6. 2000). The lectures aim at introducing essential concepts of instanton physics, with emphasis on the role of instantons in generating tunneling amplitudes, vacuum structure, and the induced quark interactions associated with the axial anomaly. A few examples for the impact of instantons on the physics of hadrons are also mentioned.

Contents

1	Introduction	2
1.1	Motivation and overview	2
1.2	WKB reminder	3
2	Instantons in quantum mechanics	4
2.1	SCA via path integrals	4
2.1.1	The propagator for real times: path integral and SCA	4
2.1.2	Propagator in imaginary time	6
2.1.3	Path integral in imaginary time: tunneling in SCA	7
2.1.4	Saddle point approximation	9
2.2	Double well (hill) potential and instantons	10
2.2.1	Instanton solution	10
2.2.2	Zero mode	12
2.2.3	Dilute instanton gas	13
2.3	Periodic potential	16
3	Instantons in QCD	18
3.1	Vacuum topology and Yang-Mills instantons	18
3.1.1	Topology of the Yang-Mills vacuum	18
3.1.2	Yang-Mills instanton solution	22
3.2	Including quarks	23
3.2.1	The axial anomaly	24
3.2.2	Quark zero modes	26
3.3	Instanton topology and theta vacua	27
3.3.1	Instanton topology and self-duality	27
3.3.2	The vacuum angle	29
4	Outlook: Instantons and hadron physics	32
4.1	Acknowledgements	34

Chapter 1

Introduction

Yang-Mills instantons were discovered a quarter of a century ago [1]. They have furnished the first explicit example of a genuinely nonperturbative gauge field configuration and display unprecedented properties rooted in topology. In fact, one could argue that the discovery of instantons marked the beginning of a new era in field theory. In the words of Sidney Coleman [2]: “In the last two years there have been astonishing developments in quantum field theory. We have obtained control over problems previously believed to be of insuperable difficulty and we have obtained deep and surprising (at least to me) insights into the structure of ... quantum chromodynamics.” Instantons have remained an active, fascinating and highly diverse research area ever since, both in mathematics and physics.

The following pages contain the notes of three elementary lectures on instantons in quantum mechanics and QCD which aim at introducing some of the underlying ideas to a non-expert audience.

1.1 Motivation and overview

QCD instantons are mediating intriguing quantum processes which shape the ground state of the strong interactions. These local and inherently nonperturbative processes can be thought of as an ongoing “re-arrangement” of the vacuum. In addition, there exist many other types of instantons in various areas of physics. This became clear shortly after their discovery when it was realized that instantons are associated with the semiclassical description of tunneling processes.

Since tunneling processes abound in quantum theory, so do instantons. We will take advantage of this situation by explaining the physical role of instantons in the simplest possible dynamical setting, namely in the one-dimensional quantum mechanics of tunneling through a potential barrier. Once the underlying physics is understood, this example can be more or less directly generalized to the tunneling processes in the QCD vacuum, where we can then concentrate on the additional complexities brought in by the field theoretical and topological aspects of Yang-Mills instantons. We will end our brief tour of instanton physics with a short section on the impact of instantons on hadron phenomenology.

As already mentioned, instantons occur in many guises and we can only give a small glimpse of this vast field here. Moreover, we will spend a large part of the available time on laying a solid conceptual foundation and will consequently have less time for applications. To do at least some justice to the diversity of the subject and to give an idea of its scope, let us mention a few actively studied topics not touched upon in these lectures: instantons have been found in many field theories, ranging from scalar field theory via supersymmetric Yang-Mills and string (or M-) theory to gravity. There are interesting relations and interactions between instantons and their topological cousins, the non-abelian monopoles and vortices. In several theories, probably including QCD, instantons are responsible for spontaneous chiral symmetry breaking. The role of instantons in deep inelastic scattering and other hard QCD processes has been examined, and also their impact on weak-interaction processes at LHC, RHIC and beyond. In inflationary cosmology and elsewhere relatives of instantons (sometimes called “bounces”) describe the “decay of the false vacuum”.

Moreover, there are fascinating mathematical developments in which instantons serve as tools. They have been instrumental, e.g., in obtaining profound results in geometry and topology, including Donaldson theory of four-manifolds (which led to the discovery of a new differentiable structures on R^4). Instantons play a particularly important role in supersymmetric gauge theories. They saturate, for example, the low-energy effective (Seiberg-Witten) action of $N = 2$ supersymmetric Yang-Mills theory.

Theoretical approaches to QCD instantons [3] include well-developed “instanton-liquid” vacuum models, a variety of hadron models at least partially based on instanton-induced interactions, a sum-rule approach based on a generalized operator product expansion (IOPE) [4], and an increasing amount of lattice simulations [5].

There is a vast literature on instantons. In preparing these lectures I have benefitted particularly from the articles and books by Coleman [2], Schulman [6], Sakita [7], Polyakov [8], Zinn-Justin [9], and Kleinert [10]. More advanced and technical work on instantons is collected in [11]. A pedagogical introduction to instantons in supersymmetric field theories can be found in [12].

The program of these lectures is as follows: first, we will discuss the semi-classical approximation (SCA) in quantum mechanics in the path integral representation. This will lead us to describe tunneling processes in imaginary time where we will encounter the simplest examples of instanton solutions. It follows a brief discussion of instantons in QCD, their topological properties and their role in generating the vacuum structure. As appropriate for a workshop on hadronic physics, we will end with a brief survey of instanton effects in hadrons as obtained from the operator product expansion of hadronic correlation functions.

1.2 WKB reminder

As we have already alluded to, instantons mediate quantum-mechanical barrier penetration processes. The semiclassical approximation (SCA) is the method of choice for the treatment of such processes. It might therefore be useful to recapitulate some basic aspects of this technique, in the form established by Wenzel, Kramers and Brioullin (WKB).

The WKB method generates approximate solutions of the Schrödinger equation for wavefunctions with typical wavelength λ small in comparison to the spacial variations of the potential. This situation corresponds to the semiclassical limit $\hbar \rightarrow 0$ since in this limit

$$\lambda = \frac{2\pi\hbar}{p} \rightarrow 0. \quad (1.1)$$

Macroscopic structures, for example, behave normally according to classical mechanics because their wavefunctions vary little compared to the variations of the microscopic potentials. The semiclassical limit is therefore the analog of the geometrical (ray) optics limit of wave optics, where the scatterers are structureless at the scales of the typical wavelengths of light.

In order to arrive at approximate solutions in the semiclassical limit, the WKB method writes the wave function as

$$\psi(x) = e^{i\Phi(x)/\hbar}. \quad (1.2)$$

Since $\Phi \in C$ this ansatz is fully general. (In scattering applications Φ is often called the “Eikonal”.) One then expands

$$\Phi(x) = \Phi_0(x) + \hbar\Phi_1(x) + \hbar^2\Phi_2(x) + \dots, \quad (1.3)$$

(this series is generally asymptotic), inserts into the Schrödinger equation, and reads off the WKB equations at a given power of \hbar by equating terms of the same order on both sides.

Although this procedure is in principle simple and intuitive, it becomes increasingly involved in more than one dimension (except for special cases [13]) and at higher orders. The generalization to many-body problems and especially to field theory is therefore often impractical (see, however, [14]). Fortunately, there is an alternative approach to the SCA, based on the path integral, which can be directly applied to field theories. With our later application to QCD in mind, we will now consider this approach in more detail.

Chapter 2

Instantons in quantum mechanics

2.1 SCA via path integrals

One of the major advantages of the path integral representation of quantum mechanics is that it embodies the probably most natural and intuitive description of the transition to classical mechanics, i.e. of the semiclassical limit. In the following chapter we will discuss this limit and the associated SCA in the simplest dynamical setting in which instantons play a role, namely in one-dimensional potential problems with one degree of freedom (a point particle, say).

2.1.1 The propagator for real times: path integral and SCA

The key object in quantum mechanics, which contains all the physical information about the system under consideration (spectrum, wavefunctions etc.), is the matrix element of the time evolution operator

$$\langle x_f | e^{-iHT_M/\hbar} | x_i \rangle, \quad (2.1)$$

i.e. the probability amplitude for the particle to propagate from

$$x_i \quad \text{at} \quad t = -\frac{T}{2} \quad \text{to} \quad x_f \quad \text{at} \quad t = \frac{T}{2}. \quad (2.2)$$

(In quantum field theory this matrix element, which is sometimes called the quantum-mechanical propagator, generalizes to the generating functional.) Its path integral representation is

$$\langle x_f | e^{-iHT/\hbar} | x_i \rangle = \mathcal{N} \int D[x] e^{i\frac{S[x]}{\hbar}} = \mathcal{N} \int D[x]_{\{x(-T/2/T/2)=x_i/x_f\}} e^{\frac{i}{\hbar} \int_{-T/2}^{T/2} dt' \mathcal{L}(x, \dot{x})}, \quad (2.3)$$

$$S[x] = \int_{-T/2}^{T/2} dt' \mathcal{L}(x, \dot{x}) = \int_{-T/2}^{T/2} dt' \left\{ \frac{m}{2} \dot{x}^2(t) - V[x(t)] \right\}, \quad (2.4)$$

where $S[x]$ is the classical action along a given path and the integration over the paths can be defined, for example, by discretization of the time coordinate (Trotter formula) as

$$D[x] := \lim_{N \rightarrow \infty} \left(\frac{mN}{2\pi i \hbar t} \right)^{1/2} \prod_{n=1}^{N-1} \left(\frac{mN}{2\pi i \hbar t} \right)^{1/2} dx_n \quad (2.5)$$

where $x_n = x(t_n)$. A for our purposes more suitable representation in terms of a complete set of functions will be introduced below.

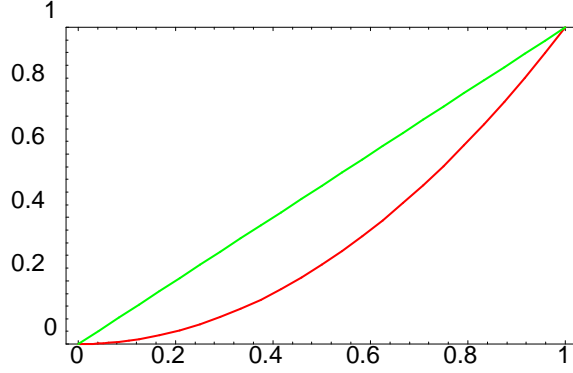


Figure 2.1: The two paths from $(x, t) = (0, 0)$ to $(1, 1)$ whose action is compared.

In the semiclassical limit, i.e. for $\hbar \rightarrow 0$, the classical action can become much larger than \hbar and the path integral is dominated by the paths in the vicinity of the stationary point(s) $x_{cl}(t)$ of the action, which satisfy

$$\frac{-\delta}{\delta x(t)} S[x] = m\ddot{x} + \frac{\partial V}{\partial x} = 0 \quad (2.6)$$

with the boundary conditions

$$x_{cl}\left(-\frac{T}{2}\right) = x_i, \quad x_{cl}\left(\frac{T}{2}\right) = x_f. \quad (2.7)$$

These classical paths are important not because they themselves give dominant contributions to the integral (in fact, their contribution vanishes since the set of classical paths is of measure zero), but rather because infinitely many neighboring paths, which lie in the so-called “coherence region” with similar phase factors $\exp(iS/\hbar)$, add coherently. For the paths outside of the coherence region the phases vary so rapidly that contributions from neighboring path interfere destructively and become irrelevant to the path integral. This exhibits in a transparent and intuitive way the relevance of the classical paths in quantum mechanics.

To get a more quantitative idea of the coherence region, let us approximately define it as the set of paths whose phases differ by less than π from the phase of the classical path (the “stationary phase”), which implies

$$\delta S[x] = S[x] - S[x_{cl}] \leq \pi\hbar. \quad (2.8)$$

Thus, for a macroscopic particle with

$$S \simeq 1 \text{ erg sec} \simeq 10^{27}\hbar \quad (2.9)$$

only an extremely small neighborhood of the classical path contributes, since $\delta\phi = \delta S/\hbar$ gets very sensitive to variations of the path. A numerical example (borrowed from Shankar [15]) makes this more explicit: compare two alternative paths from $(x, t) = (0, 0)$ to $(x, t) = (1 \text{ cm}, 1 \text{ s})$ (see Fig. ??) for a free particle: the classical path $x_{cl}(t) = t$ with $S[x_{cl}] = \int_0^T dt (m/2) v[x_{cl}]^2 = m/2$ and the alternative path $x_{alt}(t) = t^2$ with $S[x_{alt}] = 2m/3$. For a classical particle with

$$m = 1g \quad \Rightarrow \delta S = S[x_{alt}] - S[x_{cl}] \simeq 1.6 \times 10^{26}\hbar \quad \Rightarrow \delta\phi \simeq 1.6 \times 10^{26} \text{ rad} \gg \pi \quad (2.10)$$

the alternative path is extremely incoherent and therefore irrelevant, while for an electron with

$$m = 10^{-27}g \quad \Rightarrow \delta S \simeq \frac{1}{6}\hbar \quad \Rightarrow \delta\phi \simeq \frac{1}{6} \text{ rad} \ll \pi \quad (2.11)$$

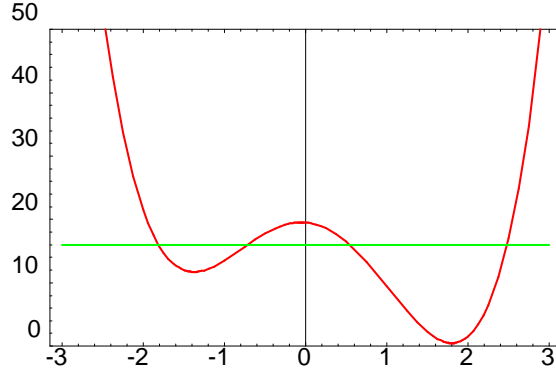


Figure 2.2: A typical tunneling potential with nondegenerate minima. The total energy (horizontal line) is smaller than the hump so that a classically forbidden region exists.

it is well within the coherence region and makes an important contribution to the path integral.

Obviously, then, the movement of a free electron cannot be described classically. One has to use quantum mechanics where the electron's path is much more uncertain and, in fact, not an observable. There also exist microscopic situations, on the other hand, where the quantum fluctuations do not totally wash out the classical results and which can therefore be treated semiclassically. A typical example is the scattering off a slowly varying potential.

However - and this is a crucial point for our subsequent discussion - the stationary-phase approximation fails to describe tunneling processes! The reason is that such processes are characterized by potentials with a classically forbidden region (or barrier) which cannot be transgressed by classical particles. In other words, there exist no classical solutions of (2.6) with boundary conditions corresponding to barrier penetration. Such a potential is shown in Fig. 2.2. As a consequence, the action $S[x]$ has no extrema with tunneling boundary conditions, and therefore the path integral (2.3) has no stationary points. Does this mean that the SCA becomes unfeasible for tunneling processes? Fortunately not, of course, as the standard WKB approximation shows. The problem is particular to the stationary-phase approximation in the path integral framework, which indeed ceases to exist. The most direct way to overcome this problem would be to generalize the familiar saddle-point approximation for ordinary integrals. This method works by deforming the integration path into the complex plane in such a way that it passes through the saddle points of the exponent in the integrand. And since there indeed exist complex solutions (related to Hamilton-Jacobi theory) of the combined equations (2.6), (2.7) in tunneling potentials, a generalization of the complex saddle-point method to integrals over complex paths would seem natural. But unfortunately integration over complex paths has not been sufficiently developed (to the best of my knowledge, although a combined approach to both diffraction and ray optics in this spirit was initiated by Keller [16], and McLaughlin [17] has performed a complex saddle point evaluation of the Fourier-transformed path integral).

However, in many instances - including our tunneling problem - an analytical continuation of the path integral to imaginary time serves the same purposes, and this is the way in which we will perform the SCA to tunneling problems in the following sections.

2.1.2 Propagator in imaginary time

As just mentioned, the paths which form the basis of the SCA to tunneling processes in the path-integral framework can be identified by analytical continuation to imaginary time. This approach was apparently first used by Langer [18] in his study of bubble formation processes at first-order phase transitions¹. In the context of the SCA, tunneling problems and instantons it was introduced by Polyakov [2].

¹Another early application of similar ideas is due to W.A. Miller [19]. (I thank Takeshi Kodama for drawing my attention to this reference.)

In order to appreciate the use of this approach, let us first see how the ground-state energy and wavefunction in tunneling situations can be obtained from the matrix element

$$Z(x_f, x_i) = \langle x_f | e^{-HT_E/\hbar} | x_i \rangle \quad (2.12)$$

which is obtained from (2.1) by analytically continuing

$$t \rightarrow -i\tau \quad (\Rightarrow T \rightarrow -iT_E) \quad (2.13)$$

(Note, incidentally, that imaginary-“time” evolution as generated by $e^{-HT_E/\hbar}$ is not unitary and therefore does not conserve probability. It might also be worthwhile to recall that the matrix element (2.12) plays a fundamental role in statistical mechanics (its trace over state space is the partition function) although this is not the angle from which we will look at it in the following.)

The matrix element $Z(x_f, x_i)$ has the energy representation

$$Z(x_f, x_i) = \sum_n e^{-E_n T/\hbar} \langle x_f | n \rangle \langle n | x_i \rangle \quad (2.14)$$

in terms of the spectrum

$$H |n\rangle = E_n |n\rangle, \quad 1 = \sum_n |n\rangle \langle n| \quad (2.15)$$

of the (static) Hamiltonian H . The energies E_n are the usual real eigenvalues, which remain unaffected by the analytical continuation. For large T the ground state dominates,

$$Z(x_f, x_i) \rightarrow e^{-E_0 T/\hbar} \langle x_f | 0 \rangle \langle 0 | x_i \rangle \quad (2.16)$$

and the ground state energy becomes

$$E_0 = -\hbar \lim_{T \rightarrow \infty} \frac{1}{T} \ln Z(x_f, x_i). \quad (2.17)$$

In order to calculate the ground state energy (and wave function) of a tunneling problem we therefore just need the $T \rightarrow \infty$ limit of the imaginary-time matrix element (2.12). In the following section we will show how to calculate this matrix element semiclassically in the path integral framework.

2.1.3 Path integral in imaginary time: tunneling in SCA

The quantum mechanical propagator (2.12) in imaginary time has a path integral representation which can be obtained from (2.3) by analytical continuation:

$$Z(x_f, x_i) = \mathcal{N} \int D[x] e^{-\frac{S_E[x]}{\hbar}} = \mathcal{N} \int D[x]_{\{x(-T/2/T/2)=x_i/x_f\}} e^{-\frac{1}{\hbar} \int_{-T/2}^{T/2} d\tau \mathcal{L}_E(x, \dot{x})}. \quad (2.18)$$

(Note, by the way, that this path integral is much better behaved than its real-time counterpart (and thus can be formalized as an integral over stochastic Wiener processes) since the oscillating integrand is replaced by an exponentially decaying one.)

For future applications it is useful to define the “measure” of this integral more explicitly. To this end, we expand $x(\tau)$ in a complete, orthonormal set of functions $\tilde{x}_n(\tau)$ around a fixed path $\bar{x}(\tau)$ as

$$x(\tau) = \bar{x}(\tau) + \eta(\tau) \quad \text{with} \quad \eta(\tau) = \sum_{n=0}^{\infty} c_n \tilde{x}_n(\tau) \quad \text{and} \quad \int_{-T/2}^{T/2} d\tau \tilde{x}_n(\tau) \tilde{x}_m(\tau) = \delta_{mn} \quad (2.19)$$

where \bar{x} itself satisfies the correct boundary conditions

$$\bar{x}(\pm T/2) = x_f/x_i, \quad (2.20)$$

$$\tilde{x}_n(\pm T/2) = 0. \quad (2.21)$$

(Note that there are no further requirements on \bar{x} .) As a consequence we have

$$D[x] = D[\eta] = \prod_n \frac{d\tilde{c}_n}{\sqrt{2\pi\hbar}}. \quad (2.22)$$

where the normalization factor is chosen for later convenience.

Now let us get the explicit form of $\mathcal{L}_E(x, \dot{x})$ (the subscript E stands for ‘‘Euclidean time’’, which is used synonymously with ‘‘imaginary time’’ in field theory) in (2.18) by analytical continuation of

$$iS = i \int_{-T/2}^{T/2} dt \left(\frac{m}{2} \dot{x}^2 - V[x] \right) \quad (2.23)$$

$$\rightarrow i(-i) \int_{-T/2}^{T/2} d\tau \left(-\frac{m}{2} \dot{x}^2 - V[x] \right) \equiv - \int_{-T/2}^{T/2} d\tau \mathcal{L}_E[x] \quad (2.24)$$

from which we read off

$$\mathcal{L}_E[x] = \frac{m}{2} \dot{x}^2 + V(x). \quad (2.25)$$

Thus, besides turning the overall factor of i in the exponent into a minus sign (as anticipated in (2.18)), the analytical continuation has the crucial implication that the potential changes its sign, i.e. that it is turned upside down!

The consequence of this for the SCA is immediate: now there exist (one or more) solutions to the imaginary-time equation of motion

$$\frac{-\delta}{\delta x(\tau)} S_E[x] = m\ddot{x}_{cl} - V'(x_{cl}) = 0 \quad (2.26)$$

with tunneling boundary conditions. These solutions correspond to a particle which starts at x_i , rolls down the hill and through the local minimum of $-V(x)$ (which corresponds to the peak of the classically forbidden barrier of $+V(x)$) and climbs up to x_f , according to the boundary conditions

$$x\left(-\frac{T}{2}\right) = x_i, \quad x\left(\frac{T}{2}\right) = x_f. \quad (2.27)$$

For later reference we note that the solutions of (2.26) carry a conserved quantum number, the ‘‘Euclidean energy’’

$$E_E = \frac{m}{2} \dot{x}^2 - V(x) \quad (2.28)$$

which follows immediately from $\dot{E}_E = \dot{x}_{cl} [m\ddot{x}_{cl} - V'(x_{cl})]$ and the equation of motion (2.26).

The essential property of these solutions in our context is that they are saddle points of the imaginary-time path integral (2.18). For $\hbar \rightarrow 0$ the only nonvanishing contributions to the path integral therefore come from a neighborhood of x_{cl} (since those are least suppressed by the Boltzmann weight $\exp(-S_E/\hbar)$) and can be calculated in saddle-point approximation.

2.1.4 Saddle point approximation

Now let us perform the saddle-point approximation explicitly. To this end we write

$$x(\tau) = x_{cl}(\tau) + \eta(\tau) \quad (2.29)$$

and expand the action around the stationary point x_{cl} (later we will sum over the contributions from all stationary points) to second order in η ,

$$S_E[x] = S_E[x_{cl}] + \frac{1}{2} \int d\tau \int d\tau' \eta(\tau) \frac{\delta^2 S_E[x_{cl}]}{\delta x(\tau) \delta x(\tau')} \eta(\tau') + (\eta^3) \quad (2.30)$$

$$= S_E[x_{cl}] + \frac{1}{2} \int_{-T/2}^{T/2} d\tau \eta(\tau) \hat{F}(x_{cl}) \eta(\tau) + (\eta^3), \quad (2.31)$$

(the first derivative vanishes since S_E is minimal at x_{cl}) where we have abbreviated the operator

$$\frac{\delta^2 S_E[x]}{\delta x(\tau) \delta x(\tau')} = \left[-m \frac{d^2}{d\tau^2} + \frac{d^2 V(x_{cl})}{dx^2} \right] \delta(\tau - \tau') \equiv \hat{F}(x_{cl}) \delta(\tau - \tau') \quad (2.32)$$

which governs the dynamics of the fluctuations around x_{cl} .

We now expand the fluctuation

$$\eta(\tau) = \sum_n c_n \tilde{x}_n(\tau) \quad (2.33)$$

in eigenfunctions of \hat{F} with

$$\hat{F}(x_{cl}) \tilde{x}_n(\tau) = \lambda_n \tilde{x}_n(\tau). \quad (2.34)$$

(\hat{F} is hermitean and bounded and thus has a complete spectrum.) For the moment we will also assume that all eigenvalues are positive, $\lambda_n > 0$. The action can then be written as

$$S_E[x] = S_E[x_{cl}] + \frac{1}{2} \sum_n \lambda_n c_n^2 + (\eta^3) \quad (2.35)$$

and

$$Z(x_f, x_i) = \mathcal{N} \int D[x] e^{-\frac{S_E[x]}{\hbar}} \simeq \mathcal{N} e^{-\frac{S_E[x_{cl}]}{\hbar}} \int D[\eta] e^{-\frac{1}{2\hbar} \int_{-T/2}^{T/2} d\tau \eta(\tau) \hat{F}(x_{cl}) \eta(\tau)} \quad (2.36)$$

Now we use (2.22) to rewrite

$$Z(x_f, x_i) = \mathcal{N} e^{-\frac{S_E[x_{cl}]}{\hbar}} \prod_n \int_{-\infty}^{\infty} \frac{dc_n}{\sqrt{2\pi\hbar}} e^{-\frac{1}{2\hbar} \sum_n \lambda_n c_n^2} \quad (2.37)$$

$$= \mathcal{N} e^{-\frac{S_E[x_{cl}]}{\hbar}} \prod_n \int_{-\infty}^{\infty} \frac{dc_n e^{-\frac{1}{2\hbar} \lambda_n c_n^2}}{\sqrt{2\pi\hbar}} \quad (2.38)$$

and obtain, after performing the Gaussian integrations,

$$Z(x_f, x_i) = \mathcal{N} e^{-\frac{S_E[x_{cl}]}{\hbar}} \prod_n \lambda_n^{-1/2} \quad (2.39)$$

$$\equiv \mathcal{N} e^{-\frac{S_E[x_{cl}]}{\hbar}} \left(\det \hat{F}[x_{cl}] \right)^{-1/2} \quad (2.40)$$

where a sum $\sum_{x_{cl}}$ is implied if there exists more than one saddle point². The formula (2.40) encapsulates the SCA to $Z(x_f, x_i)$ up to $O(\hbar)$.

Let us summarize what we have accomplished so far. The seemingly artificial analytical continuation to imaginary times has allowed us to identify those paths whose neighborhoods give the dominant contributions to the path integral in the semiclassical limit, and to evaluate this path integral to $O(\hbar)$ in the saddle-point approximation. In more physical terms the situation can be described as follows: for tunneling problems there exist no minimal-action trajectories (i.e. classical solutions) with the appropriate boundary conditions in real time. Therefore all trajectories between those boundary conditions (over which we sum in the real-time path integral) interfere highly destructively. Still, their net effect can be approximately gathered in a finite number of regions in function space, namely those in the neighborhood of the saddle points in imaginary time. In other words, while the tunneling amplitudes would have to be recovered at real times from a complex mixture of non-stationary paths (a forbidding task in practice), they are concentrated around the classical paths in imaginary time, and are therefore accessible to the saddle-point approximation. The destructive interference at real times leaves a conspicuous trace, however, namely the exponential suppression of (2.40) which is typical for tunneling amplitudes.

2.2 Double well (hill) potential and instantons

In the following sections we will apply the machinery developed above to simple tunneling problems with potentials which resemble as closely as possible the situation to be encountered later in QCD.

2.2.1 Instanton solution

Let us specialize therefore to tunneling processes between degenerate potential minima. A simple potential of the appropriate form is

$$V(x) = \frac{\alpha}{2} (x^2 - x_0^2)^2 \quad (2.42)$$

(see Fig. 2.3) which has three saddle points. Two of them are trivial (time-independent)

$$1) \quad x_{cl}(\tau) = x_0 \quad (2.43)$$

$$2) \quad x_{cl}(\tau) = -x_0 \quad (2.44)$$

and do not contribute to tunneling (since they cannot satisfy the corresponding boundary conditions; they do, however, contribute to $Z(x_0, x_0)$ or $Z(-x_0, -x_0)$). The third saddle point is due to the tunneling solution which interpolates between both maxima of $-V$:

$$x_{cl}(-T/2) = +x_0, \quad (2.45)$$

$$x_{cl}(T/2) = -x_0. \quad (2.46)$$

The above classification of solutions is common to all potentials which look qualitatively like (2.42), and all the qualitative results obtained below will apply to such potentials, too. We have specialized to (2.42) only because for this choice the tunneling solution can be obtained analytically. The easiest way to get this

²Note that we have introduced the determinant of a differential operator as the product of its eigenvalues

$$\det(\hat{O}) = \prod_n \lambda_n, \quad \hat{O}\psi_n(x) = \lambda_n\psi_n(x) \quad (2.41)$$

which generalizes the standard definition for quadratic matrices. We will not bother to give a detailed definition of such determinants (which renders the above (infinite) product finite and unique) since they will play no role in our ensuing discussion.

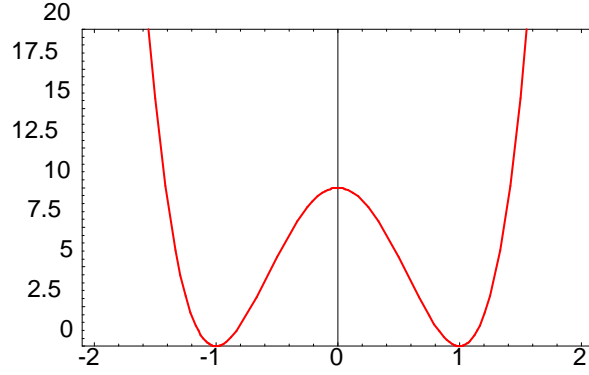


Figure 2.3: The double well potential with $\alpha = 20$ and $x_0 = 1$.

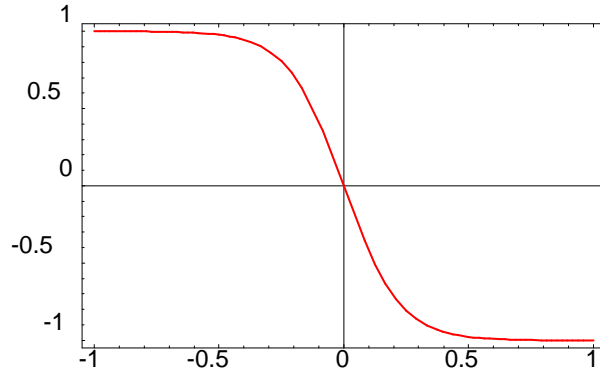


Figure 2.4: The instanton solution in the double well potential.

solution starts from the conserved Euclidean energy (2.28) with $E_E = 0$ (which corresponds to the limit $T \rightarrow \infty$ which we are interested in):

$$E_E = \frac{m}{2}\dot{x}^2 - V = 0 \quad \Rightarrow \quad \dot{x} = \sqrt{\frac{2V}{m}} \quad (2.47)$$

or, after separation of variables

$$\sqrt{\frac{m}{2}} \frac{dx}{\sqrt{V(x)}} = d\tau, \quad (2.48)$$

which can be integrated

$$\sqrt{\frac{m}{2}} \int \frac{dx}{\sqrt{V(x)}} = \sqrt{\frac{m}{\alpha}} \int \frac{dx}{x^2 - x_0^2} = \sqrt{\frac{m-1}{\alpha}} \frac{1}{x_0} \operatorname{arctan} h\left(\frac{x}{x_0}\right) = \int d\tau = \tau - \tau_0 \quad (2.49)$$

(τ_0 is the integration constant, the “position” of the instanton in imaginary time) with the result

$$3) \quad x_{cl}(\tau) \equiv x_I(\tau) = -x_0 \tanh \sqrt{\frac{\alpha}{m}} x_0 (\tau - \tau_0) \quad (2.50)$$

This solution is the **instanton** (see Fig. 2.4) of the potential (2.42). Tunneling from $-x_0$ to x_0 corresponds to the anti-instanton solution $x_{\bar{I}}(\tau) = -x_I(\tau)$. (We repeat that from the conceptual point of view there

is nothing special about the potential (2.42). Similar potentials with degenerate minima will have similar instanton solutions although those generally cannot be found analytically.)

Note that instantons are by necessity time-dependent since they have to interpolate between different minima of the potential. The name “instanton” (which goes back to ’t Hooft) indicates furthermore that the tunneling transition happens rather fast, i.e. almost instantaneous. Indeed, from the equation of motion (for $E_E = 0$)

$$\frac{dx_I}{d\tau} = \sqrt{\frac{2}{m}V(x_I)} \quad (2.51)$$

we obtain at large τ (where $V(x)$ can be expanded around x_0 with $V(x_0) = V'(x_0) = 0$ and $V''(\pm x_0) = 4Ax_0^2 \equiv \omega^2$)

$$\frac{dx_I}{d\tau} \simeq \frac{\omega}{\sqrt{m}}(x_0 \pm x_I). \quad (2.52)$$

Separating variables

$$\frac{dx_I}{x_0 - x_I} = \mp d \ln(x_0 \pm x_I) = \frac{\omega}{\sqrt{m}} d\tau \quad (2.53)$$

the asymptotic solution (for large τ) becomes

$$x_0 - x_I \rightarrow e^{-(\omega/\sqrt{m})T}. \quad (2.54)$$

Thus the instanton approaches the “vacuum value” x_0 exponentially with a characteristic time scale

$$\Delta\tau = \sqrt{m}/\omega \quad (2.55)$$

which becomes arbitrarily small for large ω . To a particle starting from $-x_0$ nothing much happens for a long time since its velocity remains almost zero. However, when it finally approaches the minimum of $-V$ it takes up speed fast, rushes through the minimum, and decelerates close to x_0 , spending all the remaining time to creep up fully and reach x_0 at $T \rightarrow \infty$.

(We note in passing that for very low tunneling barriers and correspondingly high tunneling rates (i.e. for $\omega \rightarrow 0$) semiclassical methods may fail. In such cases a variational approach sometimes turns out to be useful.)

2.2.2 Zero mode

The constant solutions 1) and 2) above share the full symmetry of the Hamiltonian H (i.e. of V). This is not the case, however, for the instanton solution since the latter is localized in imaginary time around τ_0 and therefore lacks the continuous time translation invariance of the τ -independent H . As a consequence, the instanton solutions form a continuous and degenerate one-parameter family whose members are characterized by their time-center τ_0 . In the saddle-point approximation to the path integral we have to sum (i.e. integrate) over the contributions from all τ_0 . In the present section we will see how this can be done.

To this end, let us go back to our SCA “master formula” (2.40) which was derived under the assumption $\lambda_n > 0$, i.e. for positive eigenvalues of the fluctuation operator \hat{F} . It is not difficult to see that this assumption is not valid in the case of the instanton. Since the instanton “spontaneously” breaks the time-translation symmetry of V there must be a zero mode in the spectrum of \hat{F} (for $T \rightarrow \infty$), i.e. an eigenfunction

$$\tilde{x}_0(\tau) = \sqrt{\frac{m}{S_I}} \dot{x}_I \quad (2.56)$$

(which we have normalized (at $T \rightarrow \infty$) to one:

$$\int_{-T/2}^{T/2} d\tau [\tilde{x}_0(\tau)]^2 = S_I^{-1} \int_{-T/2}^{T/2} d\tau (m\dot{x}_I^2) = 1) \quad (2.57)$$

with the eigenvalue $\lambda_0 = 0$! In order to verify that (2.56) is indeed a zero mode we have just to take a time derivative of the equation of motion (2.26):

$$m\ddot{x}_{cl} - V'(x_{cl}) = 0 \quad \Rightarrow \quad \left[m\partial_\tau^2 - V''(x_{cl}) \right] \dot{x} = -\hat{F}\dot{x} = 0 \quad \Rightarrow \quad \hat{F}\tilde{x}_0(\tau) = 0. \quad (2.58)$$

The physical origin of this zero mode is quite obvious: it corresponds to an infinitesimal shift of the instanton center τ_0 , i.e. an infinitesimal time translation of the instanton solution. Since the resulting, shifted instanton is degenerate with the original one, such a fluctuation costs no action and (2.35) implies that the corresponding eigenvalue of \hat{F} , i.e. λ_0 , must be zero.

The instanton solution (2.50) is monotonically decreasing, which implies that the zero mode satisfies $\tilde{x}_0(\tau) \leq 0$ (cf. Eq. (2.56)) and therefore has no node. As a consequence, the zero mode is the (unique) eigenfunction of \hat{F} with the lowest eigenvalue. All the remaining modes have $\lambda_n > 0$ and for them the Gaussian integrals in Eq. (2.38) are well defined. This is not the case, however, for the c_0 integration

$$\int_{-\infty}^{\infty} \frac{dc_0 e^{-\frac{1}{2\pi}\lambda_0 c_0^2}}{\sqrt{2\pi\hbar}} = \int_{-\infty}^{\infty} \frac{dc_0}{\sqrt{2\pi\hbar}}, \quad (2.59)$$

which is not Gaussian at all! And neither should it be, since τ_0 -shifting fluctuations $\eta(\tau) \sim \tilde{x}_0(\tau)$ are not damped even when they are large (i.e. for large c_0), due to the τ_0 -independence of the instanton action. The latter renders the integrand c_0 -independent and thus the integral divergent.

But this is just the kind of divergence which we should expect anyway from integrating over the infinite set of saddle points, i.e. over all τ_0 , as discussed above. Indeed, it is easy to show that

$$dc_0 \propto d\tau_0 \quad (2.60)$$

by comparing the deviations dx_I from the instanton solution which are caused by

$$\text{small time translations } \tau_0 \rightarrow \tau_0 + d\tau_0 \quad \Rightarrow \quad dx_I = \dot{x}_I d\tau_0, \quad \text{and} \quad (2.61)$$

$$\text{small coefficient shifts } c_0 \rightarrow c_0 + dc_0 \quad \Rightarrow \quad dx_I = \frac{dx_I}{dc_0} dc_0 = \tilde{x}_0 dc_0 = \sqrt{\frac{m}{S_I}} \dot{x}_I dc_0. \quad (2.62)$$

Equating both deviations gives

$$dc_0 = \sqrt{\frac{S_I}{m}} d\tau_0. \quad (2.63)$$

Thus the integration over c_0 can be done exactly and this just amounts to summing over all one-instanton saddle points³. In the presence of zero modes the expression (2.40) must therefore be replaced by

$$Z_I(-x_0, x_0) = \mathcal{N} e^{-\frac{S_E[x_I]}{\hbar}} \sqrt{\frac{S_I}{2\pi\hbar m}} T \left(\det \hat{F}[x_I]' \right)^{-1/2} \quad (2.64)$$

where the prime at the determinant indicates that λ_0 is excluded from the product of eigenvalues. Of course, the factor T in (2.64) becomes infinite in the limit $T \rightarrow \infty$ which we will take in the end. This infinity is a consequence of the infinite amount of contributing saddle points and will be cancelled by other infinities (see e.g. Eq. (2.17)), leaving the observables perfectly finite as it should be.

2.2.3 Dilute instanton gas

Up to now, we have concentrated on the saddle points corresponding to one-instanton solutions. This is not the whole story, however: there are additional (approximate) saddle points which also contribute to

³Since c_0 measures how far the instanton is collectively (i.e. simultaneously at all times) shifted in (imaginary) time, it is an example of a ‘‘collective coordinate’’.

the semiclassical tunneling amplitude. Since the instanton deviates only in a small time interval $\Delta\tau = \sqrt{m}/\omega$ sizably from x_0 or $-x_0$, and since the overlap between neighboring instantons and anti-instantons is exponentially small (cf. (2.54)), multi-(anti-)instanton solutions of (2.26) can be approximately written as a chain (i.e. a superposition) of N alternating instantons and antiinstantons, far separated in time by the (average) intervall

$$\Delta\tau = \frac{T}{N} \gg \sqrt{m}/\omega. \quad (2.65)$$

These approximate N -instanton solutions, composed of single, alternating instantons and anti-instantons at times $\tau_{0,k}$, can thus be written as

$$x_N(\tau) = \sum_{k=1}^N x_{I,\bar{I}}(\tau - \tau_{0,k}) \quad (2.66)$$

where

$$-\frac{T}{2} \ll \tau_{0,1} \ll \tau_{0,2} \dots \ll \tau_{0,N} \ll \frac{T}{2}, \quad (2.67)$$

and they have to be included as additional saddle-points in the SCA. We are now going to derive the corresponding expression for $Z(-x_0, x_0)$ in this so-called dilute instanton gas approximation (DIGA).

The contribution of the approximate N -instanton solution to the path integral is

$$Z_N \simeq \mathcal{N} \int D[\eta] e^{-S_E[x_N + \eta]/\hbar}. \quad (2.68)$$

We now write the fluctuation $\eta(\tau)$ as a sum of independent fluctuations around the single instantons and around the constant $\pm x_0$ pieces between them:

$$\eta(\tau) = \eta_0(\tau) + \sum_{k=1}^N \eta_k(\tau). \quad (2.69)$$

This implies that $\eta_0(\tau)$ can be finite all over $[-T/2, T/2]$ (except at the boundaries) while the $\eta_k(\tau)$ are time-localized around the k -th (anti-) instanton.

Hence the action approximately decomposes into the sum of actions for single (well-separated) (anti-) instantons (recall that $S[x_{cl} = \pm x_0] = 0$ and $S[x_0 + \eta] = S[-x_0 + \eta]$, due to the symmetry of the potential):

$$S_E[x_N + \eta] \simeq S_E[x_0 + \eta_0] + \sum_{k=1}^N S_E[x_I + \eta_k]. \quad (2.70)$$

This formula expresses the (approximate) fact that the (anti-) instantons have too little overlap to interact. As a consequence, Z_N factorizes as follows:

$$Z_N(-x_0, x_0) \simeq \mathcal{N} \int D[\eta_0] e^{-S_E[x_0 + \eta_0]/\hbar} \times \prod_{k=1}^N \mathcal{N} \int D[\eta_k] e^{-S_E[x_I + \eta_k]/\hbar} \quad (2.71)$$

$$= Z_0(-x_0, x_0) [Z_I(-x_0, x_0)]^N. \quad (2.72)$$

Now we do the c_0 integrations in the Z_I ,

$$Z_I = Z'_I \sqrt{\frac{S_I}{2\pi\hbar m}} \int d\tau_0 \quad (2.73)$$

and with

$$\int_{-T/2}^{T/2} d\tau_{0,1} \int_{\tau_{0,1}}^{T/2} d\tau_{0,2} \dots \int_{\tau_{0,N-1}}^{T/2} d\tau_{0,N} = \frac{T^N}{N!} \quad (2.74)$$

we arrive at

$$Z_N \simeq Z_0 \frac{(Z'_I T)^N}{N!} \quad (2.75)$$

where

$$Z_0(\pm x_0, \pm x_0) = \mathcal{N} (\det [-\partial_\tau^2 + \omega^2])^{-1/2} \rightarrow \left(\frac{\omega}{\pi\hbar}\right)^{1/2} e^{-\omega T/2} \quad (2.76)$$

for $T \rightarrow \infty$ (see [2] for the calculation of the limiting value).

In order to collect the multi-instanton contributions with different N to $Z(x_0, -x_0)$, we have to sum over all odd N (only an odd number of instantons and anti-instantons in sequence can satisfy the boundary conditions (2.45), (2.46)) and obtain

$$Z_{DIGA}(x_0, -x_0) = Z_0 \sum_{N \text{ odd}} \frac{(Z'_I T)^N}{N!} = \frac{Z_0}{2} \{e^{Z'_I T} - e^{-Z'_I T}\}. \quad (2.77)$$

(Note that the second exponential on the RHS above removes the contributions even in $Z'_I T$ and doubles those odd in $Z'_I T$). An analogous expression for $Z_{DIGA}(-x_0, -x_0)$ is obtained when only contributions from even numbers of instantons are summed. Both results can be combined in the expression

$$Z_{DIGA}(\pm x_0, -x_0) = \frac{1}{2} \left(\frac{\omega}{\pi\hbar}\right)^{1/2} e^{-\omega T/2} \{e^{Z'_I T} \mp e^{-Z'_I T}\} \quad (2.78)$$

$$= \frac{1}{2} \left(\frac{\omega}{\pi\hbar}\right)^{1/2} \left\{ e^{-(\hbar\omega/2 - \hbar Z'_I)T} \mp e^{-(\hbar\omega/2 + \hbar Z'_I)T} \right\} \quad (2.79)$$

which gives the two lowest energies of the system (i.e. those of the ground state and the first excited state) as⁴

$$E_0 = -\hbar \lim_{T \rightarrow \infty} \frac{1}{T} \ln Z_{DIGA}(\pm x_0, -x_0) = -\hbar \lim_{T \rightarrow \infty} \frac{1}{T} \left[-(\omega/2 - Z'_I)T \right] = \hbar\omega/2 - \hbar Z'_I, \quad (2.82)$$

$$E_1 = -\hbar \lim_{T \rightarrow \infty} \frac{1}{T} \left[-(\omega/2 + Z'_I)T \right] = \hbar\omega/2 + \hbar Z'_I. \quad (2.83)$$

The wave functions of the corresponding states are similarly obtained from the prefactors of the exponential in (2.79) (cf. Eq. (2.16)). As expected, we find for the ground (first excited) state the symmetric (antisymmetric) linear combinations

$$|0\rangle = \frac{1}{\sqrt{2}} \{|x_0\rangle + |-x_0\rangle\}, \quad (2.84)$$

$$|1\rangle = \frac{1}{\sqrt{2}} \{|x_0\rangle - |-x_0\rangle\}, \quad (2.85)$$

⁴We note in passing that the splitting in energy between the classical would-be ground states could have been obtained from the one-instanton approximation alone, i.e. without employing the DIGA. Indeed, restricting to small T and expanding

$$\langle x_f | e^{-HT/\hbar} | x_i \rangle = 1 - \frac{T}{\hbar} \langle x_f | H | x_i \rangle + O(T^2) \quad (2.80)$$

the propagator is governed by the (time independent) matrix element

$$\langle x_f | H | x_i \rangle \quad (2.81)$$

which can be calculated in the one-instanton approximation.

of the two “would-be” ground states $|\pm x_0\rangle$ in the absence of tunneling.

Thus we have recovered the standard WKB results for tunneling amplitudes, although in the somewhat less familiar framework of the imaginary-time path integral. The splitting of the energy levels of the states connected by tunneling is

$$\Delta E \sim e^{-\frac{S_E[x_I]}{\hbar}} \quad (2.86)$$

and the new ground state is the symmetric superposition of those states.

Before leaving this section, we should address a potential concern in summing over the dilute instanton gas in Eq. (2.77). Indeed, for an increasing number N of (anti-)instantons (in the constant interval T) the diluteness condition (2.65) is less and less satisfied, implying that from a large N onwards the corresponding terms in the sum will violate this fundamental DIGA requirement. However, Stirling’s formula $n! \simeq \left(\frac{n}{e}\right)^n \sqrt{2\pi n}$ for large n shows that the sum (2.77) is dominated by terms with

$$\frac{Z'_I T}{N} \sim O(1) \quad (2.87)$$

and that contributions from larger N are rapidly suppressed. As a consequence, only N with

$$\frac{N}{T} \lesssim C e^{-\frac{S_E[x_I]}{\hbar}}, \quad (2.88)$$

i.e. with an exponentially small instanton density in the semiclassical limit, contribute significantly to the sum (2.77). This ensures that Z_{DIGA} is dominated by terms in which the DIGA diluteness requirement (2.65) is well satisfied.

Our main motivation for the use of instanton methods in the solution of the above tunneling problem was that this solution can be straightforwardly generalized to gauge theories. In order to develop the analogy with QCD as far as possible, however, we can still go a step further in quantum mechanics by considering a periodical potential with degenerate minima. This will be the subject of the following section.

2.3 Periodic potential

Let us therefore finally consider a straightforward periodic extension of the double well potential (which thereby becomes bounded from above). This type of potential most closely resembles the situation which we will encounter below in the QCD vacuum. In a periodic potential with degenerate minima, instantons and anti-instantons can arbitrarily follow each other, connecting adjacent minima x_{0,n_i} and x_{0,n_f} , starting out at the minimum where the previous one had ended. Getting from the minimum with index n_i to the one with index n_f requires the number of anti-instantons minus the number of instantons, $N_{\bar{I}} - N_I$, to equal $n_f - n_i$. Therefore the semiclassical propagator becomes

$$Z_{per}(x_{n_f}, x_{n_i}) \simeq Z_0 \sum_{N_I=0}^{\infty} \sum_{N_{\bar{I}}=0}^{\infty} \frac{(Z'_I T)^{N_I + N_{\bar{I}}}}{N_I! N_{\bar{I}}!} \delta_{N_{\bar{I}} - N_I - (n_f - n_i)}. \quad (2.89)$$

With

$$\delta_{ab} = \int_0^{2\pi} \frac{d\theta}{2\pi} e^{i\theta(a-b)} \quad (2.90)$$

Z_{per} can be rewritten as

$$Z_{per}(x_{n_f}, x_{n_i}) \simeq Z_0 \int_0^{2\pi} \frac{d\theta}{2\pi} e^{-i\theta(n_f - n_i)} \sum_{N_I=0}^{\infty} \frac{(Z'_I T e^{i\theta})^{N_I}}{N_I!} \sum_{N_{\bar{I}}=0}^{\infty} \frac{(Z'_I T e^{-i\theta})^{N_{\bar{I}}}}{N_{\bar{I}}!} \quad (2.91)$$

$$= Z_0 \int_0^{2\pi} \frac{d\theta}{2\pi} e^{-i\theta(n_f - n_i)} e^{Z'_I T e^{i\theta}} e^{Z'_I T e^{-i\theta}} \quad (2.92)$$

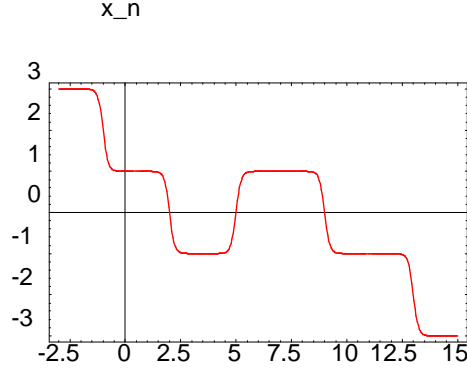


Figure 2.5: A multi-instanton solution in the periodical potential. The abscissa denotes the euclidean time τ while the ordinate gives the position variable x . The integer values of x correspond to the minima $x_{0,n}$ of the periodical potential.

and by using again the expression (2.76) for Z_0 we arrive at

$$Z_{per}(x_{n_f}, x_{n_i}) = \left(\frac{\omega}{\pi\hbar}\right)^{1/2} e^{-\omega T/2} \int_0^{2\pi} \frac{d\theta}{2\pi} e^{-i\theta(n_f - n_i)} e^{2Z'_I T \cos\theta} \quad (2.93)$$

$$= \left(\frac{\omega}{\pi\hbar}\right)^{1/2} \int_0^{2\pi} \frac{d\theta}{2\pi} e^{-i\theta(n_f - n_i)} e^{-(\omega/2 - 2Z'_I \cos\theta)T}. \quad (2.94)$$

As before, we can now obtain the ground state energy and find the θ -dependent value

$$E_0(\theta) = -\hbar \lim_{T \rightarrow \infty} \frac{1}{T} \ln Z_{per}(x_{n_f}, x_{n_i}) = -\hbar \lim_{T \rightarrow \infty} \frac{1}{T} \left[-(\omega/2 - 2Z'_I \cos\theta)T \right] = \hbar\omega/2 - 2\hbar Z'_I \cos\theta. \quad (2.95)$$

Thus the ground state energies in the periodic potential form a continuous “band”. This situation is analogous to the band of electron states in the periodic potential of a metal. Not surprisingly, then, the corresponding eigenstates are analogs of the “Bloch waves”,

$$|\theta\rangle = \frac{1}{\sqrt{2\pi}} \left(\frac{\omega}{\pi\hbar}\right)^{1/4} \sum_n e^{in\theta} |n\rangle, \quad (2.96)$$

where $|n\rangle$ is the state localized at the n -th minimum of the periodic potential.

This concludes our discussion of instantons in quantum mechanics. Much more could be said about them, their cousins (sometimes called “bounces”) which mediate tunneling between nondegenerate minima, their connections to large-order perturbation theory in the real-time theory, etc. However, we refrain from doing so since we have reached our main objective: to obtain the semiclassical expansion and the ground state properties in a potential which mimicks the situation in the QCD vacuum. We will now move on to discuss “the real thing”, namely instantons in QCD itself.

Chapter 3

Instantons in QCD

What is the relevance of the above discussion of tunneling in a periodic quantum-mechanical potential for QCD? As already anticipated, the answer is that the generalization of pertinent aspects of the SCA¹ to four-dimensional Euclidean (i.e. imaginary-time) Yang-Mills theory is straightforward once we have identified the saddle points of the classical Yang-Mills action in imaginary time. Our first task will therefore be to find the degenerate minima of the action and the corresponding tunneling solution, i.e. the Yang-Mills instanton. This will be done in the following section. We will find that the QCD instanton, a classical gluon field, possesses particular topological properties which induce physical phenomena unprecedented in the quantum mechanical examples. Some of these phenomena, including those related to the light-quark sector of QCD, will be discussed in the subsequent sections.

3.1 Vacuum topology and Yang-Mills instantons

3.1.1 Topology of the Yang-Mills vacuum

In order to develop some intuition for semiclassical ground-state properties of QCD, let us start as in the preceding quantum mechanical examples by searching for the minima of the Euclidean Yang-Mills action. Restricting for the moment to the gluon sector, the latter reads

$$S[G] = \frac{1}{4} \int d^4x [G_{\mu\nu}^a G_{\mu\nu}^a] \quad (3.1)$$

$$= \frac{1}{2} \int d^4x [E_i^a E_i^a + B_i^a B_i^a] \geq 0 \quad (3.2)$$

where the gluon field strength tensor is

$$G_{\mu\nu}(x) = \partial_\mu G_\nu - \partial_\nu G_\mu + ig [G_\mu, G_\nu] \equiv G_{\mu\nu}^a t^a, \quad t^a = \frac{\lambda^a}{2}, \quad (3.3)$$

and the chromoelectric and -magnetic fields are defined as

$$E_i^a = G_{i4}^a, \quad B_i^a = -\frac{1}{2} \varepsilon_{ijk} G_{jk}^a. \quad (3.4)$$

The corresponding quantum field theory (including the quarks) determines the structure of the QCD vacuum, i.e. the unique state of lowest energy on which the Fock space is built. Since QCD is strongly coupled

¹We note in passing that there exists a somewhat complementary way of looking at the SCA in QFT, namely as an expansion in the number of Feynman-graph loops (which exposes the non-perturbative nature of the SCA from a different angle).

and therefore non-perturbative at low energies, we expect the vacuum to be populated by strong fields. (This is in contrast to standard QED, for example, where the vacuum contains mostly zero-point fluctuations, i.e. weakly interacting electron-positron pairs and photons which can be handled perturbatively.)

A measure for the strength of the QCD vacuum fields can be obtained from the trace anomaly, which relates the energy density ϵ_{vac} of the vacuum to the phenomenologically known vacuum expectation value of the square of the gluon field strength tensor, the so-called “gluon condensate” (renormalized at about 1 GeV):

$$\epsilon_{vac} \simeq -\frac{b_1}{128\pi^2} \langle 0 | g^2 G^2 | 0 \rangle \simeq -\frac{1 \text{ GeV}}{2 \text{ fm}^3} \ll \epsilon_{pert}. \quad (3.5)$$

This relation shows that the nonperturbative vacuum fields are indeed exceptionally strong: they reduce the vacuum energy in a tiny cube of size 10^{-15}m by about half a proton mass! As we will see in the remainder of this section, part of this reduction is due to tunneling processes mediated by instantons.

Strong fields can contain a very large number of quanta, and those quanta can become coherent and render the corresponding action large compared to \hbar . In other words, such fields behave (semi-) classically since quantum fluctuations are of $O(\hbar)$ and thus contribute only relatively small corrections. The above reasoning suggests that insight into the vacuum fields of QCD may be gained from a semiclassical perspective. In the following, we will explore this perspective while paying special attention to robust and generic features which are likely to survive even stronger quantum fluctuations. The most important such features will turn out to be “global”, i.e. topological properties of the vacuum fields which are invariant under continuous deformations (and therefore in particular under time evolution).

The first step towards a semiclassical approach to the QCD vacuum (starting at the lowest order of \hbar) is to find those classical fields which minimize the (static) Yang-Mills energy or, equivalently, the Euclidean action (3.1). These fields are sometimes called “classical vacua”. Since the Euclidean action (3.1) is non-negative (in contrast to its counterpart in Minkowski space) its absolute minima will be the gluon fields with zero action. These fields are the “pure gauges”

$$G_\mu^{(pg)} = \frac{-i}{g} U \partial_\mu U^\dagger \quad (3.6)$$

where $U(x) \in SU(3)$ is an element of the gauge group. It is easy to check explicitly that the field strength of pure gauges vanishes,

$$G_{\mu\nu}^{(pg)} = 0. \quad (3.7)$$

At first sight, one might think that these fields would be natural candidates on which to build a semiclassical expansion. A moment’s reflection shows, however, that none of them could generate an acceptable vacuum since they are neither unique nor gauge invariant.

In fact, it can be easily seen that the $G_\mu^{(pg)}$ fall into an enumerable infinity of topological equivalence classes. In order to demonstrate this, we start by choosing the temporal gauge

$$G_0 = 0 \quad (3.8)$$

so that the residual gauge transformations (which conserve this gauge condition) are time-independent. Moreover, for our purposes it is useful to restrict the residual gauge transformations further by letting them approach a constant (chosen to be unity) at spacial infinity, i.e.

$$U(\vec{x}) \rightarrow 1 \quad \text{for} \quad |\vec{x}| \rightarrow \infty. \quad (3.9)$$

This restriction guarantees that the gauge fields satisfies definite boundary conditions at the surface of a large box (which should not affect the local physics inside).

The effect of the condition (3.9) is that, from the point of view of gauge transformations, the space R_{space}^3 is effectively compactified to S_{space}^3 (the 3-dimensional sphere), i.e. different boundary points at $|\vec{x}| \rightarrow \infty$ cannot be distinguished by $U(\vec{x})$ and thus can be identified. This is completely analogous to the

compactification $R^2 \rightarrow S^2$ of the complex plane by Riemann's stereographic projection. As a consequence, any residual gauge transformation $U(\vec{x})$ defines a map

$$S_{space}^3 \rightarrow SU(3)_{color}. \quad (3.10)$$

For the purpose of the following topological (homotopy) classification, this map can be furthermore restricted to a $SU(2)$ subgroup of the gauge group, since according to a powerful theorem by Raoul Bott [20] only this subgroup will be “topologically active” in our discussion. Moreover, the quaternion representation of any $U \in SU(2)$,

$$U = u_0 + iu_a\tau_a \quad \text{with} \quad u_\alpha \text{ real and} \quad u_0^2 + u_a u_a = 1, \quad (3.11)$$

(in terms of the Pauli matrices τ_a) shows that $SU(2)$ can be mapped onto the 3-sphere S_{group}^3 (which is its group manifold). Thus the map (3.10) is topologically (in the sense of homotopy theory) equivalent to

$$S_{space}^3 \rightarrow S_{group}^3 \quad (3.12)$$

i.e. any residual gauge transformation maps the spacial 3-sphere into the group 3-sphere. In general, two such mappings $U(\vec{x})$ cannot be continuously deformed into each other, which implies that they fall into different homotopy classes. The same holds for spheres of any dimension n , i.e. for any map $S^n \rightarrow S^n$.

To get a visual understanding of this topological classification, it is thus sufficient to consider just the simplest case

$$S_{sp}^1 \rightarrow S_{gr}^1 \quad (3.13)$$

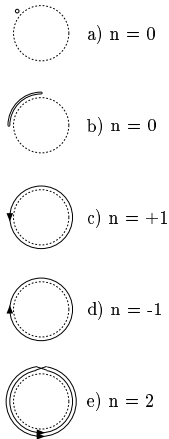
of maps between two circles. Such mappings can equivalently be thought of as phase fields $U(\chi) = e^{i\phi(\chi)} \in U(1)$ defined on a circle with coordinate angle $\chi \in [0, 2\pi]$. In Fig. 3.1 various maps of this type are graphically represented by drawing the domain space circle (which can be imagined as a rubber band) in contact with the target space (the dotted circle which represents the phase of the field) such that the mapping occurs between those points on the circles which touch each other. Note that we consider only continuous maps which implies that every point of the target circle must somewhere touch the domain circle. The examples drawn in Fig. 3.1 illustrate the topological properties of such maps. We start with Fig. 3.1a where the whole domain space shrinks to a point (which we draw as a tiny circle with radius $r \rightarrow 0$ implied) and touches the target space at one and the same point. Clearly this graph represents the constant map: all points of “space” are mapped into one and the same point in the field or target space.

Let us now consider Fig. 3.1b where the mapping (field) becomes space-dependent. We define that fields which can be continuously deformed into each other (i.e. such that the all points of the domain space stay in contact with points on the domain circle) belong to the same “homotopy class”. Now the map of Fig. 3.1b can clearly be continuously deformed into the identity map and thus belongs to the same homotopy class. This is in distinct contrast to the remaining maps of Fig. 3.1. In Fig. 3.1c the domain space wraps once counterclockwise around the target circle and therefore cannot be continuously shrunk to a point. Therefore, the corresponding map lies in a disjoint homotopy class with which we will associate a “winding number” $n = +1$. The mapping of Fig. 3.1d wraps clockwise² around the target circle and belongs to the homotopy class with winding number $n = -1$. (The trivial class containing the identity map obviously has $n = 0$.)

The next graph, Fig. 3.1e, shows a map with winding number $n = +2$ where the target space wraps twice counterclockwise around the domain space. Now it should be clear how this classification proceeds to higher winding numbers. We have thus made plausible that the maps (3.13) fall into an enumerable infinity of disjoint homotopy classes characterized by an integer winding number $n \in Z$. If one additionally defines a composition law for such maps by concatenation (under which the winding numbers of the maps to be composed simply add) the homotopy classes become elements of a group, the so-called homotopy group

$$\pi_1(S^1) = Z. \quad (3.14)$$

²Note that the direction in which a point on the curve proceeds if the curve parameter increases does not change under continuous deformations.



0-0

Figure 3.1: Some characteristic examples of the mapping $S^1 \rightarrow S^1$.

Here the subscript of π indicates the dimension of the domain sphere (in the present case equal to one), and its argument denotes the target space (here S^1). Now, according to what we have said before this result generalizes to the homotopy groups for mappings between spheres of dimension d , $\pi_d(S^d) = Z$, which includes the maps (3.12) which interest us in the context of the QCD vacuum. We thus conclude that

$$\pi_3(S^3) = Z. \quad (3.15)$$

Let us summarize what we have learned so far: the pure-gauge fields (3.6), constructed from gauge transformations $U^{(n)}(x)$ which satisfy the boundary conditions (3.9), minimize the Euclidean QCD action and fall into disjoint homotopy classes characterized by an integer winding number n which derives from the topological properties of the $U^{(n)}(x)$.

Note that the above arguments do *not* imply that we cannot transform a pure-gauge field of class n , i.e.

$$G_\mu^{(n)} = \frac{-i}{g} U^{(n)} \partial_\mu U^{(n)\dagger}, \quad (3.16)$$

by continuous deformation into one of class $m \neq n$, despite the fact that we have just shown that we cannot continuously deform $U^{(n)}$ into $U^{(m)}$. Indeed, the latter implies only that we cannot go from $G_\mu^{(n)}$ to $G_\mu^{(m)}$ without leaving pure gauge, i.e. we cannot keep the field always in the form (3.6). This also means that we cannot stay in the sector of fields with zero action (recall that the pure gauges are the only gluon fields which minimize the Euclidean action). In other words, in order to continuously deform $G_\mu^{(n)}$ into $G_\mu^{(m)}$ with $n \neq m$ we have to consider field configurations with non-minimal action, $S_E > 0$: each topological class corresponds to an absolute action minimum, and those minima are separated by finite action barriers. This situation is depicted in Fig. 3.2.

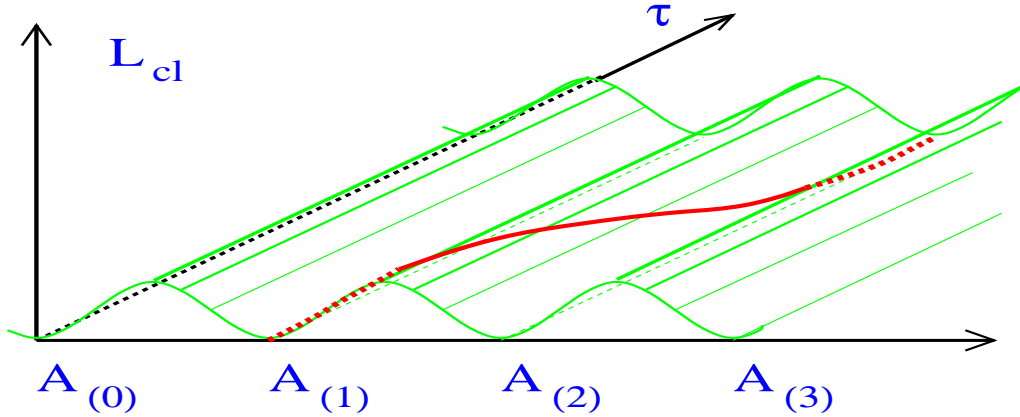


Figure 3.2: The classical, Euclidean QCD Lagrangian for different classes of gauge field configurations. The degenerate absolute minima correspond to pure gauges $A_{(n),\mu} \left(\equiv G_{\mu}^{(n)} \right)$ with winding number n . An instanton trajectory, interpolating between $A_{(1)}$ and $A_{(2)}$, is also shown.

3.1.2 Yang-Mills instanton solution

The reader has probably already noted the analogy between the degenerate classical ground state found in section 3.1.1 and the periodic potential discussed in section 2.3. In both cases, the Euclidean action has an enumerable infinity of degenerate minima. And as in the quantum mechanical examples, the degeneracy between the classical “would-be” or “candidate” vacua of QCD is lifted by tunneling of gluons through the finite action barriers.

Thus we know already, at least in principle, how to obtain the semiclassical approximation to the tunneling amplitude between the classical minima $G_{\mu}^{(n)}$: it is generated by a saddle-point approximation to the Euclidean functional integral around stationary (and approximately stationary) field configurations, i.e. the solutions of the Euclidean Yang-Mills equation

$$\frac{\delta S}{\delta G_{\nu}} = \partial_{\mu} G_{\mu\nu} + g [G_{\mu}, G_{\mu\nu}] \equiv D_{\mu} G_{\mu\nu} = 0 \quad (3.17)$$

with the boundary conditions

$$G_{\mu}(\vec{x}, T = -\infty) = G_{\mu}^{(n)}(\vec{x}), \quad (3.18)$$

$$G_{\mu}(\vec{x}, T = +\infty) = G_{\mu}^{(m)}(\vec{x}). \quad (3.19)$$

According to the above boundary conditions, the solutions start out at $T \rightarrow -\infty$ as pure-gauge fields constructed from a gauge transformation with winding number n , and they end up in a pure gauge associated with winding number m at $T \rightarrow +\infty$. Moreover, they do so with the minimal amount of action possible. These solutions are the QCD-instantons, and they can be found analytically [1, 11]. For $m = n + 1$, the instanton (in a non-singular gauge) has the explicit form

$$G_{\mu}^{(I)}(x) = \frac{2}{g} \frac{\eta_{a\mu\nu} (x_{\nu} - z_{\nu}) t^a}{(x - z)^2 + \rho^2}. \quad (3.20)$$

An instanton with $n = 1$, $m = 2$ is drawn in Fig. 3.2.

A couple of remarkable features can be read off directly from the instanton solution (3.20): first, its “spin” (i.e. the Lorentz vector index) is coupled to the color orientation by the ’t Hooft symbol $\eta_{a\mu\nu}$. Second, its nonperturbative character (as expected in the context of tunneling) reveals itself in the diverging weak-coupling limit. (The $1/g$ behavior is common to all solutions of the classical Yang-Mills equation (3.17), as

can be seen by rescaling the gluon field.) Finally, the solution makes explicit that the tunneling process is localized in a region of size ρ in space and time, around its center z .

By using the definition

$$\eta_{a\mu\nu} = \delta_{a\mu}\delta_{4\nu} - \delta_{a\nu}\delta_{4\mu} + \varepsilon_{a\mu\nu} \quad (3.21)$$

of the 't Hooft symbol, it is easy to verify that the instanton (3.20) indeed satisfies the boundary conditions (3.18), (3.19) with $n = 0$. Thus, QCD instantons describe localized, flash-like rearrangements of the vacuum which mediate tunneling processes between topologically distinct pure-gauge sectors.

In analogy with the quantum-mechanical example of the periodic potential, those tunneling processes lift the degeneracy between the pure-gauge “would-be” vacua $|n\rangle$. Instead, superpositions of all those states, the “theta vacua”

$$|0\rangle_\theta = \mathcal{N} \sum_n e^{i\theta n} |n\rangle, \quad (3.22)$$

become the gauge-invariant eigenstates. Although part of our above discussion (and of the tunneling interpretation) depended on the gauge choice (3.8), the ensuing vacuum structure is therefore gauge-independent. The emergence of the angle θ can be established even without recourse to the SCA [24]. At present, the “quantum ambiguity” implied by the a priori undetermined value of θ can only be lifted phenomenologically. This task is made easier by the fact that finite values of θ induce CP-violating amplitudes (see section 3.3.2).

Evidence from instanton-liquid vacuum models suggests that the approximate saddle points which dominate the SCA to the QCD generating functional are superpositions of instantons and anti-instantons [30, 3]. Such field configurations are approximate solutions of the Yang-Mills equation if the typical separation between the single (anti-) instantons is much larger than their average size, a condition which seems rather well satisfied in the QCD vacuum (see below). In contrast to the quantum mechanical examples of sections 2.2 and 2.3, however, the interactions between Yang-Mills instantons are of dipole type (classically and at large separations) and therefore of much longer range than the exponentially suppressed overlaps between quantum mechanical instantons (cf. Eq. (2.54)). As a consequence, the dilute instanton gas approximation fails in QCD. The stronger correlations among instantons generate an ensemble which probably resembles more a liquid than a gas. (The single- and multi-(anti-)instanton solutions by themselves play very likely a subdominant role in long-distance QCD properties.)

The size distribution $n(\rho)$ of instantons in the vacuum is currently under active investigation, mainly on the lattice [5]. The obtained results are not yet fully consistent with each other but conform more or less to the older results of instanton vacuum models [3]. (Some calculations have led to larger densities, but those are difficult to measure reliably on the lattice). For the lowest moments of the distribution, the standard values are

$$\bar{n} = \int d\rho n(\rho) \sim 1 \text{ fm}^{-4}, \quad (3.23)$$

$$\bar{\rho} = \frac{1}{\bar{n}} \int d\rho \rho n(\rho) \sim \frac{1}{3} \text{ fm}. \quad (3.24)$$

Thus, in QCD vacuum tunneling happens on average in about 5% of spacetime, and it happens very rapidly: the action barrier is penetrated almost instantaneously ($\tau_{\text{tunnel}} \sim 0.3 \times 10^{-15} \text{ m} \sim 10^{-24} \text{ s}$), therefore the name “instanton”.

3.2 Including quarks

Some of the most striking effects of QCD instantons are associated with the existence of light quarks, and not even a terse introduction to instanton physics like the present one would be complete without mentioning at least a few prominent examples. In the following two sections we will therefore try to give a flavor of the most important quark-related instanton effects.

3.2.1 The axial anomaly

Behind many essential effects of instantons in the light-quark sector stands the axial anomaly, i.e. the fact that the (flavor-singlet) axial quark current, which is conserved in the classical theory, ceases to be so at the quantum level. In the following we will derive this anomaly and some of its implications. Let us therefore switch on the fermionic part of the QCD action,

$$S_q [q, \bar{q}, G] = \int d^4x \bar{q} [i\gamma_\mu (\partial_\mu + gG_\mu)] q, \quad (3.25)$$

which couples the previously considered gluon fields to light quarks (for now we omit the quark mass term). The Noether procedure and the (Dirac) field equation imply that this action has a conserved (classical) axial current, i.e.

$$\partial_\mu (\bar{q} i\gamma_\mu \gamma_5 q) = 0. \quad (3.26)$$

Now let us compute the quantum expectation value of this current in the background of a fixed, classical gauge field G_μ , i.e.

$$J_{5,\mu} (x|G) = Z^{-1} [G] \int \mathcal{D}q \mathcal{D}\bar{q} (\bar{q} i\gamma_\mu \gamma_5 q) e^{-S_q[q,\bar{q},G]} \quad (3.27)$$

where

$$Z [G] = \int \mathcal{D}q \mathcal{D}\bar{q} e^{-S_q[q,\bar{q},G]}. \quad (3.28)$$

The (Grassmann) integration over the quark fields in (3.27) can be performed immediately with the result

$$J_{5,\mu} (x|G) = -iN_f \text{tr}_{\gamma,c} \{ \gamma_\mu \gamma_5 S(x, x|G) \} \quad (3.29)$$

(N_f is the number of quark flavors; the trace is over Dirac and color indices) which is written in terms of a Greens function $S(x, y|G)$ of the Dirac operator in the G -background, defined via

$$[i\gamma_\mu (\partial_{x,\mu} + gG_\mu(x))] S(x, y|G) = \delta^4(x - y). \quad (3.30)$$

In terms of Feynman graphs, Eq. (3.29) states that the expectation value of the axial current can be calculated from a closed quark loop in the background of a (classical) gluon field G , with one insertion of the axial vertex $\gamma_\mu \gamma_5$.

For the further evaluation of (3.29) we employ the spectral representation of $S(x, y|G)$ in terms of the eigenfunctions ψ_n of the Dirac operator \mathcal{D} ,

$$\mathcal{D}\psi_n(x) \equiv [i\gamma_\mu (\partial_\mu + gG_\mu(x))] \psi_n(x) = \lambda_n \psi_n(x), \quad (3.31)$$

(\mathcal{D} is hermitean, i.e. the spectrum is real) which reads

$$S(x, y|G) = \sum_n \frac{\psi_n(x) \bar{\psi}_n(y)}{\lambda_n}. \quad (3.32)$$

(For the moment we do not worry about vanishing eigenvalues, although they will play a prominent role later on.) In order to regularize this infinite sum we introduce a cutoff function

$$f_\varepsilon(\lambda_n^2) = e^{-\varepsilon \lambda_n^2} \quad (3.33)$$

which suppresses the contributions from large $|\lambda_n|$ and goes to unity in the limit $\varepsilon \rightarrow 0$ (which we are going to take in the end). Inserted into (3.29) this yields

$$J_{5,\mu} (x|G) = N_f \sum_n \frac{\bar{\psi}_n(x) i\gamma_\mu \gamma_5 \psi_n(x)}{\lambda_n} e^{-\varepsilon \lambda_n^2}. \quad (3.34)$$

Let us now obtain the divergence of this current by noting that (3.31) implies

$$\partial_\mu (\bar{\psi}_n i\gamma_\mu \gamma_5 \psi_n) = -2\lambda_n (\bar{\psi}_n \gamma_5 \psi_n), \quad (3.35)$$

and leads to

$$\partial_\mu J_{5,\mu}(x|G) = -2N_f \sum_n \bar{\psi}_n \gamma_5 e^{-\varepsilon\lambda_n^2} \psi_n = -2N_f \sum_n \bar{\psi}_n \gamma_5 e^{-\varepsilon\mathcal{D}^2} \psi_n = 2N_f \text{tr}_{\gamma,c} \langle x | \gamma_5 e^{-\varepsilon\mathcal{D}^2} | x \rangle \quad (3.36)$$

where

$$\mathcal{D}^2 = -(\partial_\mu + gG_\mu)^2 - \frac{g}{2}\sigma_{\mu\nu}G_{\mu\nu}. \quad (3.37)$$

We can now expand the exponential³ in powers of the classical background field G . In Feynman-diagram language, this corresponds to expanding the quark loop in the number of G insertions. Each additional G insertion implies an additional quark propagator in the loop and therefore makes the loop integral converge faster at high momenta. Thus there can be at most a few UV-divergent terms, associated with the lowest orders of G . These terms require regularization, and it is at this point where the classical axial symmetry gets broken (if we insist on keeping the vector current conserved) and the anomaly occurs.

The above reasoning is reflected in our calculation by the fact (see below) that only the leading nonvanishing term in the G expansion of (3.36) will survive the limit $\varepsilon \rightarrow 0$ which we are going to take in the end. We therefore just have to identify and calculate this single contribution. Since all the terms from the first part of (3.37) vanish due to $\text{tr}_\gamma(\gamma_5) = 0$, and since those from the first-order contribution of the second term vanish due to $\text{tr}_\gamma(\gamma_5\sigma_{\mu\nu}) = 0$, the first nonvanishing contribution originates from the second-order piece of the $\sigma_{\mu\nu}$ -term, i.e.

$$\text{tr}_{\gamma,c} \langle x | \gamma_5 e^{-\varepsilon\mathcal{D}^2} | x \rangle = \langle x | e^{\varepsilon\partial^2} | x \rangle \frac{g^2\varepsilon^2}{8} \text{tr}_\gamma(\gamma_5\sigma_{\mu\nu}\sigma_{\rho\sigma}) \text{tr}_c(G_{\mu\nu}G_{\rho\sigma}) + O(\varepsilon), \quad (3.38)$$

which corresponds to a quark loop with two interactions with the background gluon field. With

$$\text{tr}_\gamma(\gamma_5\sigma_{\mu\nu}\sigma_{\rho\sigma}) = 4\varepsilon_{\mu\nu\rho\sigma}, \quad \tilde{G}_{\mu\nu} = \frac{1}{2}\varepsilon_{\mu\nu\rho\sigma}G_{\rho\sigma} \quad (3.39)$$

and

$$\langle x | e^{\varepsilon\partial^2} | x \rangle = \int d^4p \langle x|p \rangle e^{\varepsilon\partial^2} \langle p|x \rangle = \int \frac{d^4p}{(2\pi)^4} e^{-\varepsilon p^2} = \frac{1}{16\pi^2\varepsilon^2} \quad (3.40)$$

($\langle x|p \rangle = \exp(-ip_\mu x_\mu) / (2\pi)^2$) we finally obtain (in the limit $\varepsilon \rightarrow 0$)

$$\partial_\mu J_{5,\mu}(x|G) = \frac{g^2 N_f}{8\pi^2} \text{tr}_c(G_{\mu\nu}\tilde{G}_{\mu\nu}). \quad (3.41)$$

This famous result (which can be shown to be independent of the regularization procedure) expresses the gist of the ‘‘axial anomaly’’: although the axial current is conserved in classical chromodynamics, the corresponding symmetry is broken at the quantum level, i.e. in QCD, due to the necessity of regularization and renormalization. Our discussion above followed in a somewhat abbreviated fashion Fujikawa’s approach to anomalies [21].

³Note that the G -dependence of (3.36) originates solely from the exponential since the implicit G -dependence of the ψ_n cancels in the sum. (This is because the matrix element $\langle x | \gamma_5 e^{-\varepsilon\mathcal{D}^2} | x \rangle$ is independent of the basis of functions in which one may decide to evaluate it.)

3.2.2 Quark zero modes

The existence of the axial anomaly has crucial implications for fermions in the background of instanton fields. In order to exhibit them, let us take a closer look at the Dirac spectrum

$$\mathcal{D}\psi_n(x) = \lambda_n\psi_n(x) \quad (3.42)$$

introduced in the last section. Since the (hermitean) Dirac operator anticommutes with γ_5 ,

$$\{\mathcal{D}, \gamma_5\} = 0, \quad (3.43)$$

each (normalized) eigenfunction ψ_n with $\lambda_n \neq 0$ implies the existence of another eigenfunction

$$\psi_{n,-}(x) \equiv \gamma_5\psi_n(x) \quad (3.44)$$

with eigenvalue

$$\lambda_{n,-} = -\lambda_n. \quad (3.45)$$

In other words, nonvanishing eigenvalues appear in pairs with opposite signs. The eigenfunctions $\psi_{0,k}$, corresponding to the remaining eigenvalues $\lambda_k = 0$, are called zero modes. The zero modes can be made to diagonalize γ_5 (due to (3.43)) by transforming to the chiral basis

$$\psi_{0\pm,k} = \frac{1}{2}(1 \pm \gamma_5)\psi_{0,k} \quad (3.46)$$

where

$$\gamma_5\psi_{0+,k} = +\psi_{0+,k}, \quad (3.47)$$

$$\gamma_5\psi_{0-,k} = -\psi_{0-,k}. \quad (3.48)$$

Since, finally, the QCD Dirac operator is flavor-independent, i.e.

$$[\mathcal{D}, \mathcal{T}_a] = 0, \quad (3.49)$$

(the \mathcal{T}_a are generators of the flavor group) each zero mode comes in N_f copies (one of each flavor).

The two main properties of the Dirac spectrum established above (paired eigenvalues of opposite sign and chiral zero modes) have profound consequences. One of those becomes explicit by integrating the anomaly equation (3.41) over space-time and using Eq. (3.36) (multiplied by a factor $1/(2N_f)$) to write

$$Q \equiv \frac{g^2}{16\pi^2} \int d^4x \text{tr}_c(G_{\mu\nu}\tilde{G}_{\mu\nu}) \quad (3.50)$$

$$= - \sum_n e^{-\varepsilon\lambda_n^2} \int d^4x \bar{\psi}_n \gamma_5 \psi_n. \quad (3.51)$$

Above we have defined the ‘‘topological charge’’ Q whose meaning will be clarified below. Since the eigenfunctions ψ_n and $\gamma_5\psi_n$ of \mathcal{D} have different eigenvalues (λ_n and $-\lambda_n$) and are thus orthogonal to each other, the integral in (3.51) vanishes for all n with $\lambda_n \neq 0$, leaving us with an integral over the zero modes $\psi_{0,k}$:

$$Q = - \sum_k \int d^4x \bar{\psi}_{0,k} \gamma_5 \psi_{0,k} \quad (3.52)$$

$$= \sum_{m=1}^{n_-} \int d^4x \bar{\psi}_{0-,m} \psi_{0-,m} - \sum_{m=1}^{n_+} \int d^4x \bar{\psi}_{0+,m} \psi_{0+,m} \quad (3.53)$$

where n_{\pm} is the number of right- (left-) handed zero modes in the given background gluon field. Since the eigenfunctions of \mathcal{D} (including the zero modes) are normalized, we finally obtain

$$Q = n_- - n_+. \quad (3.54)$$

The above formula, relating a topological property Q of the gauge field to the number of unpaired quark zero modes of the Dirac operator (3.31) in its background, is a special case of the celebrated Atiyah–Singer index theorem [22, 23] for the Dirac operator.

3.3 Instanton topology and theta vacua

So far, we have established two important features of the axial anomaly: first, in order for the anomaly to have physical relevance there must be gauge fields with non-vanishing topological charge Q , and second, such fields imply the existence of unpaired zero modes in the spectrum of the corresponding Dirac operator. Our next tasks will be to better understand the topological charge and to find gluon fields which carry it.

3.3.1 Instanton topology and self-duality

We start by noting that the integrand of the topological charge Q (cf. (3.50)) can be written as a total derivative

$$\frac{g^2}{16\pi^2} \text{tr}_c (G_{\mu\nu} \tilde{G}_{\mu\nu}) = \partial_\mu K_\mu \quad (3.55)$$

(we do not need the explicit expression for the ‘‘Chern-Simons current’’ K_μ here), which implies that only fields with nontrivial behavior at the boundary $x^2 \rightarrow \infty$ (typical for topologically active fields) can carry a finite Q . Furthermore, the index theorem (3.54) implies that Q can only take integer values and cannot therefore change under continuous deformations of the gluon background field. Thus, besides the homotopy classification of the pure gauges encountered in section 3.1.1, gluon fields can carry another nontrivial topological property, Q . As we have seen above, fields with nonvanishing Q ‘‘activate’’ the anomaly (cf. (3.41)) by generating quark zero-modes and are therefore associated with a non-conservation of the axial charge $q_{ax}(\tau) = \int d^3x J_{5,4}(x|G)$:

$$Q = \frac{g^2}{16\pi^2} \int d^4x \text{tr}_c (G_{\mu\nu} \tilde{G}_{\mu\nu}) = \frac{1}{2N_f} \int d^4x \partial_\mu J_{5,\mu}(x|G) = \frac{1}{2N_f} \int d\sigma_\mu J_{5,\mu}(x|G) \quad (3.56)$$

$$= \frac{1}{2N_f} \int d^3x J_{5,4}(x|G) \Big|_{\tau=-\infty}^{\tau=\infty} = \frac{1}{2N_f} [q_{ax}(\tau = \infty) - q_{ax}(\tau = -\infty)]. \quad (3.57)$$

We will now show that an integer value of Q can be assigned to any gluon field with finite (Euclidean) action (only those are relevant for the SCA), and that this value has a transparent physical interpretation. For the action (3.1) to be finite, the field strength has to be square integrable, i.e. it must vanish at the boundary $S^3(x^2 = \infty)$ of Euclidean space: $G_{\mu\nu} \rightarrow 0$ faster than $1/x^2$ for $x \rightarrow \infty$. Now we know from section 3.1.1 that the Euclidean action has its absolute minimum at $G_{\mu\nu} = 0$, so that finite-action fields satisfy the boundary condition

$$\lim_{x^2 \rightarrow \infty} G_\mu = \frac{-i}{g} U^{(n)}(x) \partial_\mu U^{(n)-1}(x), \quad (3.58)$$

where U is an element of the gauge group \mathcal{G} . We note that the instantons, which interpolate between pure gauges of different winding numbers $n(\tau = -\infty) \neq n(\tau = +\infty)$, are of this type (cf. (3.18), (3.19)).

The essential consequence of Eq. (3.58) is that it implies a time-independent topological classification of all finite-action gauge fields. This classification is based on (but not equal to) the homotopy analysis of the

gauge group elements $U^{(n)}$ which we have already encountered in section 3.1.1. Indeed, Eq. (3.58) implies that any finite-action gauge field defines a map $S^3(x^2 = \infty) \rightarrow \mathcal{G}$, and such maps fall into disjoint homotopy classes according to the third homotopy group⁴ $\pi_3(\mathcal{G})$ of \mathcal{G} . For $\mathcal{G} = SU(N)$ with $N \geq 2$, which includes QCD, we have as in section 3.1.1 $\pi_3(SU(N)) = Z$ (while, e.g., (non-compact) QED has $\pi_3(U(1)) = 0$). As a consequence, all finite-action gluon fields in Euclidean QCD fall into topologically distinct classes. It can be shown that these classes are labeled by the topological charge Q (which is technically the ‘‘Pontryagin index’’ of the gauge field)⁵.

For instantons, the topological charge Q has a particularly transparent meaning: it is just the difference between the winding numbers n and m of the pure gauges between which the instanton interpolates,

$$Q = m - n. \quad (3.59)$$

Instead of proving this expression in general (which would not be difficult), let us check it for the explicit instanton solution (3.20) found above. We first calculate the (classical) instanton action (from which we know already that it is finite and that it is minimal in its Q -sector) by plugging the field strength

$$G_{I,\mu\nu}(x) = \frac{-4\rho^2}{g} \frac{\eta_{a\mu\nu} t_a}{[(x-x_0)^2 + \rho^2]^2} \quad (3.60)$$

(obtained by inserting the expression (3.20) for the instanton into the general expression (3.3) for the Yang-Mills field strength tensor) into the Yang-Mills action (3.1). The result is

$$S_I = \frac{1}{2} \int d^4x \text{tr}_c(G_{I,\mu\nu} G_{I,\mu\nu}) = \frac{8\pi^2}{g^2}. \quad (3.61)$$

We note that the classical action is additive for (multi-)(anti-)instantons, $S_Q = |Q| \times S_I$, and that it does not depend on the instanton’s collective coordinates z_μ , U and ρ . The latter is a direct consequence of the translation, gauge, and scale invariance of classical Yang-Mills theory. At the quantum level, the scale invariance gets broken by the trace anomaly (yet another variety of anomaly) and the effective quantum action becomes ρ -dependent. This generates a ρ -dependent weight $n(\rho)$ in functional integrals which can be identified with the instanton size density introduced at the end of section 3.1.1.

Having calculated the instanton action, we can now easily check whether the instanton has indeed $Q = 1$. Inspection of the field strength (3.60) reveals that it depends on the Lorentz indices only via the ‘t Hooft symbol (3.21). Moreover, the definition (3.21) implies that

$$\frac{1}{2} \varepsilon_{\rho\sigma\mu\nu} \eta_{a\mu\nu} = \eta_{a\rho\sigma}. \quad (3.62)$$

which shows that the field strength of the instanton is self-dual,

$$G_{I,\mu\nu} = \tilde{G}_{I,\mu\nu}. \quad (3.63)$$

(Above we have used the definition (3.39) of the dual field strength \tilde{G} .) The self-duality of the instanton implies

$$Q_I = \frac{g^2}{16\pi^2} \int d^4x \text{tr}_c(G_{I,\mu\nu} \tilde{G}_{I,\mu\nu}) = \frac{g^2}{16\pi^2} \int d^4x \text{tr}_c(G_{I,\mu\nu} G_{I,\mu\nu}) = \frac{g^2}{8\pi^2} S_I = 1. \quad (3.64)$$

(The anti-instanton is anti-selfdual, i.e. $G_{\bar{I},\mu\nu} = -\tilde{G}_{\bar{I},\mu\nu}$, and thus has $Q_{\bar{I}} = -1$.) (Anti-) Self-duality is a mathematically very powerful property. Self-dual fields satisfy, for instance, automatically the Yang-Mills equation (3.17). This is an immediate consequence of the Bianchi identity

$$D_\mu \tilde{G}_{\mu\nu} = 0 \quad (3.65)$$

⁴In mathematical terms, $\pi_3(\mathcal{G})$ classifies principal \mathcal{G} fibre bundles over S^4 [23].

⁵At this point, it might be useful to emphasize the differences between the topological classification discussed here and that of the pure gauges in section 3.1.1. The winding number n of the latter classifies maps from compactified space S^3_{space} into the gauge group (and applies only to static, pure gauges), while Q characterizes maps from the boundary S^3 of Euclidean spacetime into the gauge group.

which holds for any gauge field, due to the form (3.3) of the field strength tensor. In practice, this is often advantageous since Eq. (3.63) is of first order and therefore easier to solve than the Yang-Mills equation itself. As a matter of fact, the original instanton solution was found in [1] by solving (3.63). Similarly, in the quantum mechanical example of section 2.2.1 we derived the instanton solution by solving the corresponding first-order equation (2.47). Self-duality also has powerful mathematical implications on a deeper level, e.g. in Donaldson theory. It can be shown, incidentally, that all (local) minima of the Euclidean Yang-Mills action are self-dual, and that they correspond to (multi-) instanton solutions [11].

From the index theorem (3.54) we conclude that there must be one unpaired zero-mode per flavor in an instanton field with $Q = 1$. The corresponding eigenfunctions ψ_0 can be obtained analytically (they are left-handed for the instanton and right-handed for the anti-instanton) and inherit several characteristic features of the instanton, including the localization in space and time and the coupling of spin and color. These zero modes generate the dominant instanton effects in the light-quark sector. They also induce interactions between instantons.

The integrated anomaly equation (3.57) reveals that the $Q = 1$ instanton is accompanied by the creation of $2N_f$ units of axial charge. This process is mediated by zero-mode-generated, non-local $2N_f$ -quark interactions which are known as 't Hooft vertices [25]. As a reflection of the anomaly, these vertices manifestly break the axial $U(1)$ symmetry of the QCD lagrangian (with zero quark masses) and thereby provide the (at least qualitative) resolution of the so-called “ $U(1)$ problem”, i.e. they explain why the η' meson has almost twice the mass of the η meson and cannot be considered a (quasi) Goldstone boson. The 't Hooft interaction has a characteristic channel dependence (it is, e.g., strongly attractive in spin-0 quark-antiquark and glueball channels, but generates no interaction in the vector and axial-vector channels) which is reflected in instanton-induced contributions to hadronic amplitudes. We will come back to this issue in the final chapter of these lectures.

3.3.2 The vacuum angle

In the following section we will elaborate on the instanton-induced vacuum structure which we have anticipated in section 3.1.1 by exploiting the analogy with the periodic potential. There are several angles from which one can see the structure of the theta vacuum (and the implied quantum ambiguity) emerge. One possibility is to start from the requirement of a gauge invariant vacuum state. This condition is most conveniently implemented in the Schrödinger wave functional framework where one imposes Gauss' law (in operator form) to be satisfied on the vacuum functional. This approach provides a more general derivation (independent of the SCA) of our earlier observation that the topological “would-be” vacua $|n\rangle$ are gauge-dependent and that their superposition (with a θ -dependent phase), the theta vacuum

$$|0\rangle = \mathcal{N} \sum_n e^{i\theta n} |n\rangle, \quad (3.66)$$

is the gauge-invariant ground state.

Below we will follow a different line of reasoning which goes back to the original work on theta vacua [26]. It starts from the cluster-decomposition requirement for QCD amplitudes and gives, as a side benefit, additional insights into the role of instantons in the path integral and in physical amplitudes. In particular, this approach provides an answer for the question of how the different topological charge sectors should be treated in the functional integral over the gluon fields. In fact, it was not clear a priori whether one should, for example, treat different Q -sectors independently by restricting the functional integration to selected values of Q (like the $Q = 0$ sector in which perturbation theory takes place). Or do all sectors have to be included, and if so, with what weights? Interestingly, these questions can be answered by ensuring the cluster decomposition principle⁶, which formalizes the requirement that distant measurements yield uncorrelated results, to hold.

At the Greens function level, the cluster decomposition principle requires that (connected, time-ordered) expectation values of products of local operators at distant positions factorize. Let us see what this implies

⁶The cluster decomposition principle is one of the basic requirements on any physically sensible, local quantum field theory. It can be shown to hold under rather general conditions on the form of the Hamiltonian, see [27].

for the vacuum expectation value of an operator $\mathcal{O}[q, \bar{q}, G]$ which is composed of QCD fields and which we assume to be strongly localized in a spacetime volume Ω_1 . (In other words, \mathcal{O} has support only in a small volume inside Ω_1 .) We split the total (Euclidean) spacetime volume Ω as $\Omega = \Omega_1 + \Omega_2$ and write

$$\langle 0 | \mathcal{O} | 0 \rangle_\Omega = \frac{\sum_{Q=-\infty}^{\infty} w(Q) \int \mathcal{D}q \mathcal{D}\bar{q} \mathcal{D}G_Q \mathcal{O}[q, \bar{q}, G] e^{-S[q, \bar{q}, G, \Omega]}}{\sum_{Q=-\infty}^{\infty} w(Q) \int \mathcal{D}q \mathcal{D}\bar{q} \mathcal{D}G_Q e^{-S[q, \bar{q}, G, \Omega]}} \quad (3.67)$$

where we have kept an open mind on the question of which Q -sectors to include by implementing the most general case, i.e. by summing the contributions of all topological charge sectors with a yet to be determined weight function $w(Q)$ (which may be zero for some Q). Now we note that the topological charge Q of a gluon field in the total volume Ω may be written as a sum $Q = Q_1 + Q_2$ over its topological charges Q_1 in Ω_1 and Q_2 in Ω_2 (where $Q_{1,2}$ do not have to be integer since the condition (3.58) only holds at the boundary of Ω). The action is additive, too, $S[\Omega] = S[\Omega_1] + S[\Omega_2]$, and the functional “measure” over any field ϕ on Ω factorizes as

$$\int \mathcal{D}\phi_\Omega = \prod_{x \in \Omega} \int d\phi(x) = \prod_{x_1 \in \Omega_1} \int d\phi(x_1) \prod_{x_s \in \Omega_s} \int d\phi(x_s) = \int \mathcal{D}\phi_{\Omega_1} \times \int \mathcal{D}\phi_{\Omega_2}. \quad (3.68)$$

Thus we can rewrite the above matrix element as

$$\langle 0 | \mathcal{O} | 0 \rangle_\Omega = \frac{\sum_{Q_1, Q_2} w(Q_1 + Q_2) \int [\mathcal{D}q \mathcal{D}\bar{q} \mathcal{D}G_{Q_1}]_{\Omega_1} \mathcal{O}[q, \bar{q}, G_{Q_1}] e^{-S[\Omega_1]} \times \int [\mathcal{D}q \mathcal{D}\bar{q} \mathcal{D}G_{Q_2}]_{\Omega_2} e^{-S[\Omega_2]}}{\sum_{Q_1, Q_2} w(Q_1 + Q_2) \int [\mathcal{D}q \mathcal{D}\bar{q} \mathcal{D}G_{Q_1}]_{\Omega_1} e^{-S[\Omega_1]} \times \int [\mathcal{D}q \mathcal{D}\bar{q} \mathcal{D}G_{Q_2}]_{\Omega_2} e^{-S[\Omega_2]}}. \quad (3.69)$$

(Note that the overcounting due to the double sum cancels between numerator and denominator.)

Since the operator \mathcal{O} is strongly localized in Ω_1 , cluster decomposition requires that $\langle \mathcal{O} \rangle$ must be independent of what is going on in the far separated volume Ω_2 . This is the case only if

$$w(Q_1 + Q_2) = w(Q_1) w(Q_2) \quad \Rightarrow \quad w(Q) = e^{iQ\theta} \quad (3.70)$$

with a real, free parameter θ . As a consequence, (3.69) reduces to

$$\langle 0 | \mathcal{O} | 0 \rangle_\Omega = \frac{\sum_Q e^{iQ\theta} \int \mathcal{D}q \mathcal{D}\bar{q} \mathcal{D}G_Q \mathcal{O}[q, \bar{q}, G_Q] e^{-S[\Omega_1]}}{\sum_Q e^{i\theta Q} \int \mathcal{D}q \mathcal{D}\bar{q} \mathcal{D}G_Q e^{-S[\Omega_1]}}, \quad (3.71)$$

which shows that we indeed have to integrate over the gluon fields of all topological charge sectors, with a given, θ -dependent weight. Incidentally, the above θ -dependence is exactly what one would expect for matrix elements of gauge-invariant operators between the θ -vacuum states (3.66):

$$\langle 0 | \mathcal{O} | 0 \rangle = \frac{\sum_{m,n} e^{in\theta} e^{-im\theta} \langle m | \mathcal{O} | n \rangle}{\sum_{m,n} e^{in\theta} e^{-im\theta} \langle m | n \rangle} \quad (3.72)$$

$$= \frac{\sum_Q e^{i\theta Q} [\sum_n \langle n + Q | \mathcal{O} | n \rangle]}{\sum_Q e^{i\theta Q} [\sum_n \langle n + Q | n \rangle]}, \quad (3.73)$$

where the expressions in the square brackets collect the matrix elements which connect pure-gauge sectors with winding number difference Q , just as the functional integrals in Eq. (3.71).

In order to bring (3.71) into a more familiar form, we define

$$\sum_Q \mathcal{D}G_Q \equiv \mathcal{D}G, \quad S'_{QCD} \equiv S_{QCD} - iQ\theta, \quad (3.74)$$

and then have

$$\langle 0 | \mathcal{O} | 0 \rangle = \frac{\int \mathcal{D}q \mathcal{D}\bar{q} \mathcal{D}G \mathcal{O}[q, \bar{q}, G] e^{-S'_{QCD}}}{\int \mathcal{D}q \mathcal{D}\bar{q} \mathcal{D}G e^{-S'_{QCD}}}. \quad (3.75)$$

Analytically continuing back to Minkowski space (with $d^4x_E = id^4x_M$, $G_{a34} = -iG_{a30}$, $\varepsilon^{0123} = +1$) and recalling Eq. (3.50), the generalized action (3.74) becomes

$$S'_{QCD,M} = S_{QCD,M} - \frac{\theta g^2}{16\pi^2} \int d^4x \text{tr}_c \left(G_{\mu\nu} \tilde{G}^{\mu\nu} \right) \quad (3.76)$$

which amounts to adding the term

$$\mathcal{L}_\theta = -\frac{\theta g^2}{16\pi^2} \text{tr}_c \left(G_{\mu\nu} \tilde{G}^{\mu\nu} \right) \quad (3.77)$$

to the QCD lagrangian (in Minkowski space). This new (renormalizable) interaction had been discarded during the initial development of QCD since it is a total derivative (cf. (3.55)). The latter implies that it plays no role in perturbation theory (perturbative excitations of the vacuum have $Q = 0$), in the field equations, and more generally for globally trivial fields. Only the later discovery of instantons showed explicitly that this term can have physical consequences, the most dramatic being strong CP violation. Indeed, (3.77) breaks the combined charge conjugation (C) and parity (P) (or, equivalently, time-reversal) symmetry of the QCD lagrangian.

The physical realization of strong CP violation does not depend solely on \mathcal{L}_θ , however. This can be seen by invoking a flavor-dependent chiral $U(1)$ redefinition

$$q_f \rightarrow e^{i\alpha_f \gamma_5} q_f \quad (3.78)$$

of the quark field of flavor f in the functional integral. Due to the axial anomaly, such a chiral transformation produces a nontrivial change in the measure of the quark fields, which effects a shift in the value of θ :

$$\theta \rightarrow \theta + 2 \sum_f \alpha_f. \quad (3.79)$$

(This can be shown by arguments almost identical to those of section 3.2.1.) Since the quark mass term

$$\mathcal{L}_m = -\frac{1}{2} \sum_f [m_f \bar{q}_f (1 + \gamma_5) q_f + m_f^* \bar{q}_f (1 - \gamma_5) q_f], \quad (3.80)$$

written here in its most general, CP and T non-conserving form with complex “mass” parameters m_f (note that for real m_f the γ_5 part vanishes and the standard (CP-even) mass term reemerges), explicitly breaks chiral invariance, it also changes under (3.78). This change amounts to

$$m_f \rightarrow e^{2i\alpha_f} m_f. \quad (3.81)$$

Since a redefinition of the path integration variables is not allowed to change physical properties, the latter can depend only on the invariant combination

$$e^{-i\theta} \prod_f m_f \equiv e^{-i\bar{\theta}} \prod_f |m_f| \quad (3.82)$$

of θ and the mass parameters m_f , or equivalently on

$$\bar{\theta} = \theta - \sum_f \arg(m_f). \quad (3.83)$$

Eq. (3.82) shows that a finite θ would have no observable consequences (no CP violation, in particular) if at least one quark mass would be zero. (Although this seems quite unlikely in QCD, it cannot be firmly ruled out at present.)

From the experimental bounds on the (CP-violating) dipole moment of the neutron we know that $\bar{\theta}$ has to be exceedingly small⁷, $\bar{\theta} < 10^{-9}$. How can the two seemingly independent terms in (3.83) cancel so (almost) perfectly? The unknown physical mechanism behind this cancellation and the unexplained smallness of $\bar{\theta}$ are referred to as the “strong CP problem”. Several theoretical ideas for its solution [28], most prominently the axion models, have been proposed.

⁷ or very close to $\bar{\theta} = \pi$

Chapter 4

Outlook: Instantons and hadron physics

We are coming to the end of these lectures and still have barely scratched the surface of instanton physics. This was to be expected, given the extent and variety of this field. However, in a workshop on hadronic physics it would hardly be appropriate to close the discussion without having given at least a glimpse of what impact instantons have on hadrons.

We have argued above that instantons play an essential role in shaping the QCD vacuum. And, together with other intense, strongly correlated vacuum fields, they render this ground state truly complex. As a case in point, the “elementary excitations” of such ground states are typically not the canonical degrees of freedom in which we formulate the microscopic dynamics (in QCD the quarks and gluons) but rather bound states or “collective” degrees of freedom (in QCD the hadrons) which can be considered as disturbances of the vacuum “medium”.

Condensed-matter physics supplies many interesting examples of such composite elementary excitations. One of them is the propagation of phonons in a crystal: the properties of phonon spectra and wave functions are intimately linked to the structure of the underlying crystal ground state (e.g. to its geometry, its distance scales, the interactions between the specific ions, etc.). As a consequence, a thorough understanding of excitation (phonon) properties (beyond simple mean-field approximations à la Debye) requires detailed knowledge of the ground state. Practically all quantum systems with many degrees of freedom share this requirement, and QCD is very likely no exception. Thus, knowing an important ingredient of the QCD vacuum wave functional, the instantons, it is natural to ask what this knowledge implies for hadron structure.

This question is difficult to answer since interacting instanton ensembles, strongly coupled to other vacuum fields over large distances, do not lend themselves easily to a systematic and model-independent treatment (this is common to just about any infrared-sensitive problem in QCD). As a consequence, unequivocal and quantitative evidence for instanton effects in hadrons turned out to be difficult to establish and the role of instantons in hadronic physics has remained elusive until long after their discovery.

Nonetheless, several complementary approaches have inbetween significantly improved our theoretical understanding of this role. One of the first lines of attack was to include instanton-induced interactions into hadron models (like MIT-bag and quark-soliton models) [29]. Instanton vacuum models [3, 30] start at a more fundamental level and approach the physics of the instanton ensemble by approximating the field content of the vacuum solely as a superposition of instantons and anti-instantons. This approach, which neglects other (including perturbative) vacuum fields, has been developed for almost two decades and can describe an impressive amount of hadron phenomenology (from static properties and correlation functions to parton distributions [3, 31]).

As we have already noted, QCD lattice simulations recently began to complement such vacuum model studies by isolating instantons in equilibrated lattice configurations and by studying their size distribution and their impact on hadron correlators [5]. While results obtained from different, currently developed lattice

techniques have not yet reached quantitative agreement, they do confirm the overall importance of instantons and some bulk properties of their distribution in the vacuum. However, despite some initial attempts it will still take considerable time and effort before these numerically intensive simulations can establish reliable links to hadron structure. Moreover, lattice “measurements” usually do not give insight into the physical mechanisms which generate their data. For such purposes it is useful to resort to more transparent, analytical approaches.

Over the last years, I have been involved in the development of such an approach, which has the capacity to relate the instanton component of the vacuum rather directly to hadron properties [4]. This largely model-independent method has led to several qualitative and quantitative insights into the role which instantons play in hadronic physics. Some of those I will now briefly discuss.

The central idea is to calculate hadronic correlations functions

$$\Pi_{1,\dots,n}(x_1, \dots, x_n) = \langle 0 | T J_1(x_1) J_2(x_2) \cdots J_n(x_n) | 0 \rangle, \quad (4.1)$$

i.e. vacuum expectation values of hadronic currents $J(x)$ (these are composite QCD operators with hadron quantum numbers, e.g. $J_M(x) = \bar{q}(x)\Gamma q(x)$ for mesons) at short, spacelike distances by means of a generalized operator product expansion which systematically implements instanton contributions (IOPE). The pivotal merit of this expansion is that it factorizes (at short distances $|x_i| \ll \Lambda_{QCD}^{-1}$) the contributions of all field modes to (4.1) into soft ones (with momenta below a given “operator renormalization scale” μ , $k_i < \mu$) and hard ones ($k_i \geq \mu$). The soft contributions, from instantons as well as from other soft vacuum fields, are summarily accounted for by vacuum expectation values of colorless operators (the “condensates”), while the hard contributions, originating from perturbative fluctuations and from small (or “direct”) instantons, are calculated explicitly. Input are the phenomenologically known values of a few condensates and of the two bulk properties (3.23) and (3.24) of the instanton distribution. On this basis, the IOPE provides a model-independent, controlled approximation to the correlation functions at distances $|x| \lesssim 0.2 - 0.3$ fm. In particular, it achieves a unified QCD treatment of instanton contributions in conjunction with contributions from long-wavelength vacuum fields and perturbative fluctuations.

Hadron properties are obtained from the IOPE by matching it to a dual, hadronic description of the correlators. The latter is based on a parametrization of the corresponding spectral functions in terms of hadron properties and local quark-hadron duality (which is essentially a consequence of asymptotic freedom). The specifics of the matching between both descriptions rely on techniques developed for QCD sum rules (like e.g. the use of the Borel transform) [33]. While the application range of the IOPE approach is smaller than that of instanton vacuum model and lattice calculations, it has the advantages of being transparent, largely model-independent and fully analytical.

Over the last years several hadronic channels have been studied in this framework, including those of pions [34, 35], baryons [32, 36, 37, 38] and glueballs [39]. In addition to quantitative predictions for hadron properties, these investigations have led to various qualitative insights into how instantons manifest themselves in hadron structure:

1. In several hadron channels the direct instanton contributions were found to be of substantial size and impact. This adds to the evidence from other sources for the importance of instantons in hadron structure. More specifically, the results show that nonperturbative effects can strongly affect hadron structure already at surprisingly small distances $|x| < 0.2$ fm, and that most of these effects can be attributed to (semi-hard) instantons.
2. Instanton effects are strongly hadron-channel selective and favor especially spin-0 meson and glueball channels. Moreover, various invariant amplitudes of the same correlator can receive qualitatively and quantitatively different instanton contributions. In such situations the neglect of hard instantons (which is standard practice in conventional QCD sum rules) leads to reduced stability or failure of those sum rules which are more strongly affected by instantons. Implementing the missing direct-instanton contributions led, in particular, to the resolution of long-standing stability problems in the chirally-odd nucleon sum-rule [32], one of the magnetic-moment sum rules [37], and the (lowest moment) scalar glueball sum rule [39].

3. Stable and predictive IOPE-based sum rules exist even for correlators which do not permit a conventional QCD sum rule analysis. In particular, the first sum rule for the pion form-factor based on pseudoscalar currents could be established in the IOPE approach [34]. Its prediction for the form-factor agrees well with experiment in the full range of accessible momentum transfers.
4. Instanton effects enhance the magnetic susceptibility of the quark condensate. The resulting values are in line with predictions of other, independent approaches. Moreover, direct instantons have a strong impact on one of the magnetic-moment sum rules of the nucleon and considerably improves their overall stability and consistency [37].
5. An interesting new mechanism for instanton-enhanced isospin-breaking in hadrons was found in [36]. Although instantons, being gluon fields, are “flavor blind”, they can strongly amplify isospin violation effects which originate from other, soft vacuum fields (most prominently from the difference of the up- and down-quark condensate) and which manifest themselves, e.g., in the proton neutron mass difference. Even sophisticated quark models which include instanton-induced quark interactions miss such effects.
6. The scalar glueball can be (over-) bound by the instanton contributions alone [39]. In fact, this channel provides the first example for a sum rule which can be stabilized solely by the contributions from instantons. This result lends support to the findings of instanton vacuum models [40] which neglect the remaining contributions. Incidentally, a mainly instanton-bound 0^{++} glueball fits naturally to the particularly small glueball radius r_G found on the lattice [41], which is of the order of the instanton size:

$$r_G \sim \bar{\rho}. \quad (4.2)$$

The IOPE also provides the first set of 0^{++} glueball sum rules which are overall consistent with the low-energy theorem which governs the zero-momentum limit of the corresponding correlator [39].

7. Direct instantons generate by far the dominant contributions to the IOPE of the scalar glueball correlator. This makes it possible to establish approximate scaling relations between the bulk features of the instanton distribution and the mass m_G and decay constant f_G of the scalar glueball [39]:

$$m_G \sim \bar{\rho}^{-1}, \quad (4.3)$$

$$f_G^2 \sim \bar{n} \bar{\rho}^2. \quad (4.4)$$

These relations are the first of their kind and provide a particularly direct link between instanton and hadron properties.

The above findings, together with those from other sources, are beginning to assemble into a comprehensive picture of how instantons manifest themselves in hadron structure and interactions. This picture will certainly become richer and more detailed in the future, incorporating physics ranging from nuclear and quark matter to hard processes, and it will very likely also teach us more about how to deal with nonperturbative QCD in general.

4.1 Acknowledgements

It is a pleasure to thank the organizer, Prof. Yojiro Hama, for this pleasant and informative workshop and Profs. Krein and Chiapparini for the invitation to lecture on instantons.

Bibliography

- [1] A.A. Belavin, A.M. Polyakov, A.S. Schwartz, and Yu.S. Tyupkin, Phys. Lett. **B59**, 85 (1975).
- [2] S. Coleman, in *The Ways of Subnuclear Physics*, Ed. A. Zichichi (Plenum, New York, 1977).
- [3] T. Schäfer and E.V. Shuryak, Rev. Mod. Phys. **70**, 323 (1998).
- [4] H. Forkel, *Instantons, OPE and Hadron Structure*, to be published.
- [5] See, for example, M.C. Chu and S. Huang, Phys. Rev. D **45**, 2446 (1992); M.-C. Chu, J.M. Grandy, S. Huang and J. Negele, Phys. Rev. D **49**, 6039 (1993); P. van Baal, Nucl. Phys. Proc. Suppl. **63**, 126 (1998); D.A. Smith and M.J. Teper, Phys. Rev. D **58**, 014505 (1998); A. Hasenfratz and C. Nieter, Nucl. Phys. Proc. Suppl. **73**, 503 (1999); M. Teper, OUTP-9945P, hep-lat/9909124; I.-O. Stamatescu, hep-lat/0002005.
- [6] L.S. Schulman, *Techniques and Applications of Path Integration* (John Wiley, New York, 1981, 1996).
- [7] B. Sakita, *Quantum Theory of Many-Variable Systems and Fields* (World Scientific, Singapore, 1985).
- [8] A.M. Polyakov, *Gauge Fields and Strings* (Harwood, London, 1987).
- [9] J. Zinn-Justin, *Quantum Field Theory and Critical Phenomena* (Clarendon, Oxford, 1989).
- [10] H. Kleinert, *Pfadintegrale* (BI Wissenschaftsverlag, Mannheim, 1993).
- [11] *Instantons in Gauge Theory*, Ed. M.A. Shifman (World Scientific, Singapore, 1994).
- [12] M.A. Shifman and A.I. Vainshtein, *Instantons versus supersymmetry*, in *ITEP Lectures on Particle Physics and Field Theory* (World Scientific, Singapore, 1999).
- [13] P.L. Kapur, Proc. Roy. Soc. A163, 535 (1937); P.L. Kapur and R. Peierls, Proc. Roy. Soc. A163, 606 (1937); Proc. Roy. Soc. A166, 277 (1938).
- [14] J.L. Gervais and B. Sakita, Phys. Rev. **D16**, 3507 (1977).
- [15] R. Shankar, *Principles of Quantum Mechanics*, 2nd edition (Plenum, New York, 1994).
- [16] J.B. Keller, J. Opt. Soc. Amer. **52** 116 (1962).
- [17] D.W. McLaughlin, J. Math. Phys. **13**, 1099 (1972).
- [18] J.S. Langer, Ann. Phys. **41**, 108 (1967); **54**, 1762 (1969).
- [19] W.A. Miller, Adv. Chem. Phys. **25**, 69 (1974).
- [20] R. Bott, Bull. Soc. Math. France **84**, 251 (1956).
- [21] K. Fujikawa, Phys. Rev. Lett. **42**, 1195 (1979); Phys. Rev. **D21**, 2848 (1980).
- [22] M. Atiyah and I. Singer, Ann. Math. **87**, 484 (1968).

- [23] C. Nash, *Differential Topology and Quantum Field Theory* (Academic Press, London, 1991).
- [24] See, e.g. R. Jackiw in *Lectures on QCD, Foundations* (Springer, Berlin, 1997).
- [25] G. 't Hooft, Phys. Rev. **D 14**, 3432 (1976).
- [26] C.G. Callan, R.F. Dashen, and D.J. Gross, Phys. Lett. **63B**, 334 (1976).
- [27] S. Weinberg, *The Quantum Theory of Fields, Vol. I* (Cambridge University Press, Cambridge, 1995).
- [28] R.D. Peccei, in *CP Violation*, Ed. C. Jarlskog (World Scientific, Singapore, 1991).
- [29] D. Horn and S. Yankielowicz, Phys. Lett. **B76**, 343 (1978); W.U. Blask, U. Bohn, M. Huber, B. Metsch, and H. Petry, Z. Phys. A **337**, 327 (1990); A.E. Dorokhov, Y.A. Zubov, and N.I. Kochelev, Sov. J. Part. Nucl. **23**, 522 (1992); A. Christov et al., Prog. Part. Nucl. Phys. **37**, 91 (1996).
- [30] D. I. Diakonov and V. Yu. Petrov, Nucl. Phys. **B245**, 259 (1984); Phys. Lett. **B147**, 351 (1984); Nucl. Phys. **B272**, 457 (1986).
- [31] D. I. Diakonov and V. Yu. Petrov, NORDITA preprint 2000/76 NP, hep-ph/0009006.
- [32] H. Forkel and M.K. Banerjee, Phys. Rev. Lett. **71**, 484 (1993).
- [33] M. A. Shifman, A. I. Vainshtein and V. I. Zakharov, Nucl. Phys. **B147**, 385, 448 (1979).
- [34] H. Forkel and M. Nielsen, Phys. Lett. **B 345**, 55 (1995).
- [35] H. Forkel, Heidelberg preprint HD-TVP-00-12 (2000).
- [36] H. Forkel and M. Nielsen, Phys. Rev. **D 55**, 1471 (1997).
- [37] M. Aw, M.K. Banerjee and H. Forkel, Phys. Lett. **B 454**, 147 (1999).
- [38] H. Forkel, to be published.
- [39] H. Forkel, Heidelberg preprint HD-TVP-00-1 (2000), hep-ph/0005004.
- [40] T. Schaefer and E.V. Shuryak, Phys. Rev. Lett. **75**, 1707 (1995).
- [41] P. de Forcrand and K.-F. Liu, Phys. Rev. Lett. **69**, 245 (1992); R. Gupta et al., Phys. Rev. D **43**, 2301 (1991).